

12-2016

Removal of Carboxylic Acids and Water from Pyrolysis Oil

George Alexander Marshall
University of Arkansas, Fayetteville

Follow this and additional works at: <http://scholarworks.uark.edu/etd>

 Part of the [Petroleum Engineering Commons](#)

Recommended Citation

Marshall, George Alexander, "Removal of Carboxylic Acids and Water from Pyrolysis Oil" (2016). *Theses and Dissertations*. 1811.
<http://scholarworks.uark.edu/etd/1811>

This Thesis is brought to you for free and open access by ScholarWorks@UARK. It has been accepted for inclusion in Theses and Dissertations by an authorized administrator of ScholarWorks@UARK. For more information, please contact scholar@uark.edu, ccmiddle@uark.edu.

Removal of Carboxylic Acids and Water from Pyrolysis Oil

A thesis submitted in partial fulfillment
of the requirements for the degree of
Master of Science in Chemical Engineering

by

George A. Marshall
University of Arkansas
Bachelor of Science in Chemical Engineering, 2014

December 2016
University of Arkansas

This thesis is approved for recommendation to the Graduate Council.

Professor Jamie Hestekin, Ph. D.
Thesis Director

Adjunct Professor Yupo Lin, Ph.D.
Committee Member

Professor Michael Ackerson, Ph.D.
Committee Member

Professor Robert Beitle, Ph. D.
Committee Member

Abstract

Over 70% of the world's energy consumption is provided by fossil fuels and with those reserves depleting at a fast rate, alternative energy sources or methods are needed to support the world's energy needs. This research was done in an attempt to make it more economically feasible to produce fuel products, such as bio-diesel, from the upgrading of bio-oil obtained from the pyrolysis of biomass waste material such as sawdust. The high water and oxygenated compound content of bio-oil make it undesirable for fuel use; however, two methods involving surface modified commercial membranes were utilized in hopes of overcoming these problems: electro dialysis and a pressure-driven system. Nafion 117 membrane pores were expanded and then the membrane was subjected to bio-oil at pressures up to 700 psi with the goal of removing the water. Although the pores were enlarged, removing water through this method was unsuccessful. Electro dialysis was used in an effort to remove carboxylic acids from bio-oil, which are known to cause storage instability. The membranes used for this separation were Neosepta CMX and AMX commercial membranes. Modifications to the AMX membrane surface were made by adding crosslinked polyethylenimine groups to the surface of the membrane and its performance was compared to that of the unmodified one. A XPS and FTIR analysis proved the modified membrane to be more resistant to bio-fouling.

© 2016 by George A. Marshall
All Rights Reserved

Acknowledgements

The completion of this thesis would not have been possible without the help and support of family, friends, and faculty at the University of Arkansas. First and foremost, I would like to thank my advisor Dr. Jamie Hestekin for sharing his experience, knowledge, and insight on membrane separation processes. Dr. Hestekin has guided me through this experience with patience and support and I have learned a lot from him. I would like to thank Process Dynamics Inc. and Argonne National Lab for funding my research. I would also like to thank my co-advisor Dr. Michael Ackerson, Blake Johnson, and the scientists at Process Dynamics Inc. for allowing me to use the facility if needed and for the opportunity to get involved in the bio-oil production process. I would like to thank Dr. Yupu Lin at Argonne National lab for the guidance provided to me in running electro dialysis experiments. I am grateful for Dr. Dmytro Demidov for his assistance in sample analysis and ordering chemicals. I would also like to thank my dear friend Ms. Vicky Tori for the home cooked meals and couch she provided for me to sleep on. And finally, I would like to thank my family for their continual support and encouragement through this whole experience, you all were my motivation in completing my degree.

Table of Contents

I. Introduction	1
A. Problem and proposed solution.....	2
II. Theoretical Concept	3
A. Bio-oil properties.....	5
B. Bio-oil production.....	8
III. Safety, storage, and handling	12
IV. Experimental	13
A. Membrane modification for pressure-driven separation.....	14
B. Pressure-driven experiment procedure.....	19
Sepa cell 2 set-up.....	20
Experimental Set-up/procedure.....	22
C. Membrane modification for electro-dialysis (ED).....	24
D. Electro-dialysis procedure.....	25
Glass cell set-up.....	25
ED experimental procedure.....	28
V. Analysis	29
A. Membrane pore size.....	30
Method.....	31
Results.....	32
B. Water concentration determination.....	35
Method.....	36
Results.....	38
C. Conductivity and pH.....	40
Method.....	40
Results.....	40
D. Membrane surface characterization.....	47
Method.....	48
Results.....	48
VI. Conclusion	53
VII. Literature Cited	55
VIII. Appendix	60
A. KF raw results.....	60
B. Evaporometry equations.....	62
C. Bio-oil GC/MS.....	64
D. HPLC results.....	68
E. Sample Microscopies.....	70
F. Karl Fischer titration Standard Operating Procedure (SOP).....	73

I. Introduction

With depleting fossil fuel reserves, bio-oil is gaining a considerable amount of attention as a potential energy source, partly due to the several advantages of using bio-oil over fossil fuels. One advantage of using bio-oils is that it is greenhouse gas neutral (1), meaning the overall amount of greenhouse gasses: carbon dioxide and carbon monoxide, does not increase in the atmosphere upon combustion. In fact, the bio-char byproduct of the production of pyrolysis oil may even help with carbon sequestration (2). Other advantages of using bio-oil as an energy source is that it does not emit sulfur oxides and also has a lower emission of nitrogen oxides than that of fossil fuels (3). This favors bio-oil in that it can aid with the reduction of at least two criteria air pollutants the Environmental protection agency is striving to regulate and reduce (4). Given that virtually all organic matter can be pyrolyzed (3), and the fact that the 2.3 billion acres of United States (US) land are comprised of approximately 52% of agricultural land and 35% of grazing area which is mostly grassland pasture and grazed forests (5), there is a potential in energy feedstock security as opposed to the present system. Though bio-oil seems to be a promising replacement for fossil fuels, its water content and other oxygenated organic compounds give it inferior fuel properties and cause, during storage, its degradation over time.

Bio-oil is a mixture of hundreds of different compounds which, upon separation, can be used in many different applications. In ancient times, Egyptians used pyrolysis to make tar for caulking boats and as an embalming agent (6); pyrolysis was also used to make charcoal (7). Nowadays, not only may it be used as a fuel, but bio-oil components may also and in fact are being used by some industries. For example, Red Arrow Inc. produces smoke flavor and browning agents from the lightest water-soluble fraction of bio-oil (8). Some of the carboxylic acids in bio-oil may also be useful in a variety of different industries, e.g., acetic acid, which is used to make acetates in

the food industry (9). Formic acid is used in the textile industry and has been found to have some therapeutic uses (9). Propionic acid is used in the plastic and perfume industries and butyric and heptanoic acids are used for synthesis of esters for food aromas (9). Ongoing research has been targeted at removing the water and other relatively small oxygenated compounds to improve fuel and storage properties, and possibly aiding in economic feasibility of the bio-oil upgrading process by being able to sell extracted compounds to industries such as those discussed above.

A. Problem and proposed solution

The research for this thesis was aimed at finding a solution for decreasing the undesirable properties of bio-oil due to the water and oxygenated organic compounds found in it; this was done through the use of surface modified commercial membranes. Two different processes were used for this research, a pressure-driven system where nanofiltration pore size membranes were used and electro dialysis which used anion and cation exchange membranes. Figure 1 displays where the proposed solution would fit in the sawdust to fuel conversion process.

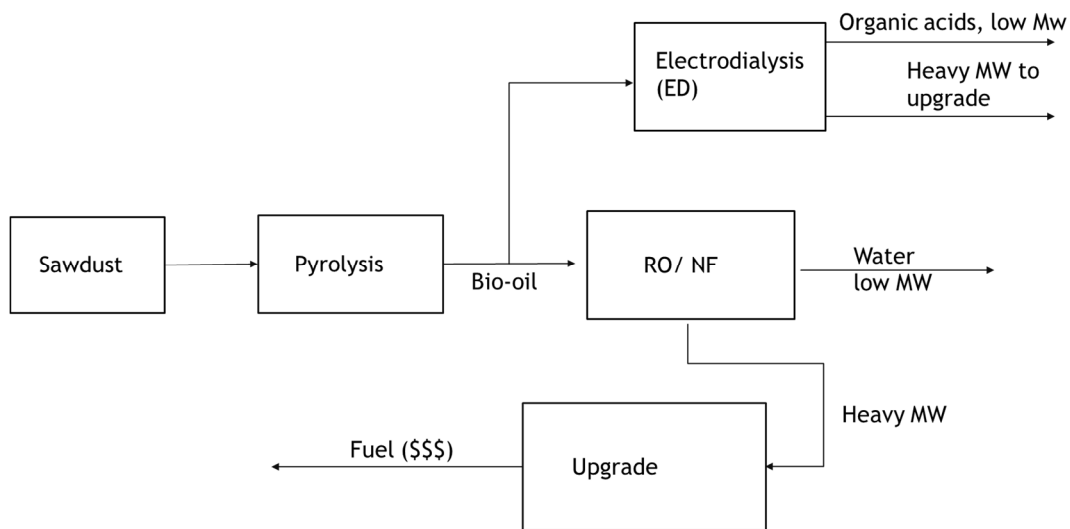


Figure 1. Proposed sawdust to fuel process modification.

II. Theoretical

Pyrolysis is the thermochemical decomposition, in the absence of oxygen, of large complex hydrocarbons in biomass to smaller simpler molecular products of gas, liquid, and char.

Pyrolysis involves rapid heating and the temperature range at which it is carried out depends on the desired product; 300-650°C is used for liquid, 800-1000°C for gas, and 200-300°C for char

(2). The initial product is made of condensable gasses, non-condensable gasses, and solid char (10). Non-condensable gasses produced are known as syngas and include carbon monoxide, carbon dioxide, hydrogen, and other light molecular weight gasses like methane (10). The other gasses are condensed to give pyrolysis oil, an oxygenated compound comprised of water and water insoluble compounds which is referred to as pyrolytic lignin because it comes from the lignin part of the biomass. Bio-oil is a complex mixture of water and hundreds of organic compounds belonging to several different categories, such as acids, aldehydes, ketones, alcohols, esters, anhydrosugars, furans, phenols, guaiacols, syringols, nitrogen compounds, and large molecular oligomers (11).

The main organic components in biomasses can be classified as cellulose, hemicellulose, and lignin. Each component by itself gives a different amount of pyrolysis products. Cellulose reactions mainly lead to liquid formation and gives yields greater than 80% (12). Lignin is reported to produce mostly char instead of bio-oil while the pyrolysis of hemicellulose gives bio-oil yields somewhere between the two other components (11). The amount of these components differs from one type of biomass to another. Woods, for example, have an average cellulose composition of 41-43% and 20-35% hemicellulose (13), while cotton is almost pure α -cellulose (14). The components have different, though slightly overlapping, decomposition temperatures shown below in table 1.

Table 1 (15). decomposition temperatures of Cellulose, Hemicellulose, and Lignin.

<u>Component</u>	<u>Decomposition Temperature range</u>
Cellulose	240-350 °C
Hemicellulose	200-260 °C
Lignin	280-500 °C

Biomass conversion to bio-oil and bio-oil composition vary with feedstock, feedstock moisture, and process conditions such as vapor residence time, temperature, and heating rate (2). Since multiple variables affect the bio-oil composition, understanding the amount of reactions and their mechanisms have been proven difficult. For this reason, studies on lumped kinetic parameters for simplified models are more common than those for bio-oil compound production (16). There are several kinetic modeling techniques that describe the generation of pyrolysis products from biomasses. Liden et al. (16) classifies three ways to model the pyrolysis reaction, which are listed below:

1. The global kinetic models which are used to determine the decomposition rate of a starting biomass by means of measuring weight loss.
2. The general kinetic model of measuring the kinetic parameters for the formation of general products such as tar, gas, and/or char.
3. The specific product approach traces the formation of a specific compound of interest from a starting material of the biomass used. This approach attempts to take into consideration secondary reactions that may occur between volatile product intermediates.

The first two above have proven to be relatively successful in establishing kinetic parameters (16, 17, 18, 19). An example of a lumped parameter model is the one done by Liden et al. (16) wherein the pyrolysis of wood feedstocks were assumed to be two first order reactions to give

products of the liquid tar and char with gas. The tar was then assumed to undergo a secondary reaction to produce more gas.

Model predictions from this lump parameter approach have been proven to yield relatively good results. The approach of modeling specific compounds is expected to be a complex network of reactions, including but not limited to, a number of simultaneous secondary reactions. Reaction parameters for these types of reactions in pyrolysis were not found but proposed reaction schemes for cellulose and hemicellulose were published by Shen et al. (13, 20). These reaction schemes only describe those of cellulose and hemicellulose; no mechanism has been found proposing a mechanism for lignin. Cellulose decomposition was reported to undergo an initial activation step before proceeding to one of two reaction pathways, either a ring scission reaction or depolymerization (21). Hemicelluloses are reported to be mostly xylans and glucomannans and the proposed decomposition mechanism shows the formation scheme for some carboxylic acids, reinforcing the idea the acids in bio-oil from fast pyrolysis are mainly produced from the degradation of hemicellulose (22).

A. Bio-oil properties

Due to high oxygenation of bio-oil, it is insoluble in hydrocarbons and its elemental composition of is similar to that of its parent biomass (10). Organic acid formation due to biomass degradation gives bio-oil a pH of about 2 to 3 and a typical water content of 15-35%, but it may be much higher depending on the initial biomass moisture. In bio-oil, water is dissolved or exists as an emulsion (23). A phase separation is known to occur at water levels of 30-45% (10).

Pyrolysis oil heating values are about half (about 26 MJ/kg) of the heavy fuel oil values of 42-44 MJ/kg; it also contains less nitrogen, metals, and sulfur than heavy fuel oils (10). Compounds in

char can act as catalysts for many reactions that increase water, ester, hydrates, ethers, oligomers and resins. Polymerization may also occur, which can increase viscosity and reduce the solubility in the bio-oil, thus causing suspended particles, emulsions, or phase separations. Bio-oils with lower char contents tend to have lower aging rates (24). Bio-oil contains less than 0.5 wt% solid char, typically, with an average particle size of approximately 5 μm when cyclone(s) are used to remove char from the hot product during pyrolysis. Fast pyrolysis produces typically about 12 wt% char as a by-product from bark-free wood (23).

Blends of bio-oil with other fuel sources such as alcohols have been proven to have improved fuel properties compared to the pure bio-oil and are hence more likely to be easier to get it into the energy market than its pure form (25).

Material compatibility of bio-oil is important to determining the appropriate pump, storage tank, hoses and gaskets, injectors, and/or valves, depending what will be done with the bio-oil. Plastics such as Teflon (polytetrafluoroethylene), PP (polypropylene), polyester resins and HDPE (high density polyethylene) are resistant to bio-oil and may serve as storage and transportation containers, with Teflon being the most resistant and PP the least (23). Other common materials such as Viton, Buna-N, and EPDM (Ethylene Propylene Diene Monomer rubber) undergo volume expansions up to 100% (23, 26). This was partly supported by the findings of Naranjo et al. (25) who exposed a variety of materials to bio-oil/bio-ethanol blends and measured reduced hardness of both Viton and SBR (Styrene Butadiene Rubber) when exposed to the bio-oil blend for times greater than 672 hours. The hardness of synthetic plastics such as PP, PE, and PVC was not affected but the breaking strength and elongation values were.

Several metals have also been tested for compatibility with bio-oil. Fuleki et al. (27) tested brass, aluminum, mild and stainless steel by exposing them bio-oil for a duration of 360 hours at different temperatures: room temperature, 50°C, and 70°C. It was concluded that the mild stainless steel and aluminum were susceptible to a considerable amount of corrosion and hence were not compatible with the bio-oil tested, which had a pH of 2.4 and water concentration of 19% (27). Soltes and Lin also concluded that aluminum and mild steel were incompatible with bio-oil, they claimed it corroded both (28). Although, by the end of the experiment, the brass and austenitic stainless steel had experienced negligible weight change, the author warns that these were static conditions and there may be some deviance from these results in dynamic fuel systems, where the softness of brass may be susceptible to erosion from particulate matter (27). Kirk et al. (26) concluded that stainless steels such as the 304L, 316L, 430, and 20M04 are suitable to use with bio-oil. It should be noted that some metals showed discrepancies between their elevated temperature and room temperature analysis. This can be seen in the low chromium alloy steels, which showed good resistance at room temperature but, at the elevated temperatures, it showed considerable corrosion (26).

Due to the nature of bio-oil and its incompatibility with certain materials, research has been done testing bio-oil on modified power generators. Bio-oil has been tested with modified gas turbines, diesel, co-firing, and Stirling engines, but there is still much work that needs to be done to implement bio-oil into industrial power generation. Bio-oil heating values lie between 16 to 26 MJ/kg (10), while other sources such as gasoline, diesel, crude oil, and methane have values of 44-46, 45, 42-44, and 50 MJ/kg, respectively. Due to bio-oil complexity and the fact that its properties differ drastically with differing variables such as feedstock and process conditions, there is a need for standardized tests of the bio-oil fuel properties. This lead to the approval of

the ASTM D7544, which covers grades of biofuel produced from biomass intended for use in various types of fuel burning equipment operating at different conditions (29). Two different grades of biofuel that may be used are listed along with required specifications such as density, water content, solids content, and gross heat of combustion. It should be noted that the two grades are intended for industrial burners designed for these specifications and not commercial residential burners.

There are several methods known to improve the fuel properties of bio-oil, one of which is hydrogenation, which is an established method for petroleum refining that has been adapted for use with bio-oil. The problem with this method is that the catalyst used is subject to a significant amount of coking, which affects the quality of fuel. Other upgrading processes may require the use of expensive equipment and/or solvents to the point where fuel production from bio-oil is not economically feasible. Achieving the separation of water and carboxylic acids by the means of a membrane may help in reducing the cost of upgrading through the sale of the carboxylic acids and less hydrogen consumption in hydrogenation.

B. Bio-oil production

Bio-oil for this research was produced by Process Dynamics Inc. in Fayetteville, AR with a pilot plant consisting of an auger reactor using stainless steel buck shot as the heat transfer agent. The auger reactor consists of two insulated compartments, each with its own auger, 96 inches long with a 3-inch pitch. One compartment is used to react the biomass, sawdust in this case, and other is used as a shot return. This is a continuous process with a feed rate of 82.9 g/min. The reactor is heated by means of a 1 by 120-inch heating tape delivering approximately 1570 W. Operating temperatures for bio-oil production ranged from 700°F (371°C) to 1000°F (538°C) and

the residence time from 3-4 seconds. The reactor experienced a slight vacuum of 1.5 in H₂O and the carrier gas was nitrogen.

Dry sawdust was added to a hopper, which fed the biomass into the reactor; once the biomass was pyrolyzed, the gas stream produced, consisting of condensable, non-condensable, and biochar as well as nitrogen, was then subjected to a cyclone to remove the biochar from the gaseous stream. This stream was then quenched via direct contact with cold kerosene by means of sprayers, causing most of the condensable gasses to condense, and the stream was pulled into a bio-oil decanting tank which also had a cold kerosene sprayer that further quenched the gaseous stream. The resulting gaseous stream was then pulled either to the atmosphere, during the beginning of the run, or to a mixer which had kerosene mixing into it which aided in the quenching process to condense the more of the condensables. The bio-oil collection tanks were designed to exploit the immiscibility of kerosene and bio-oil. The bio-oil would settle at the bottom and the kerosene would pour onto a separated section of the vessel once the liquid level would get high enough, this section transports the kerosene to a cold trap to get cooled and reused again. The bio-oil is periodically collected from the bottom of these tanks and added back into the kerosene cooling system. A close representation of the separating mechanism in the bio-oil collection tank is shown in figure 2 below; it should be noted that neither nitrogen nor the small amounts of bio-char that may have not been captured by the cyclone are considered in the following figures and tables.

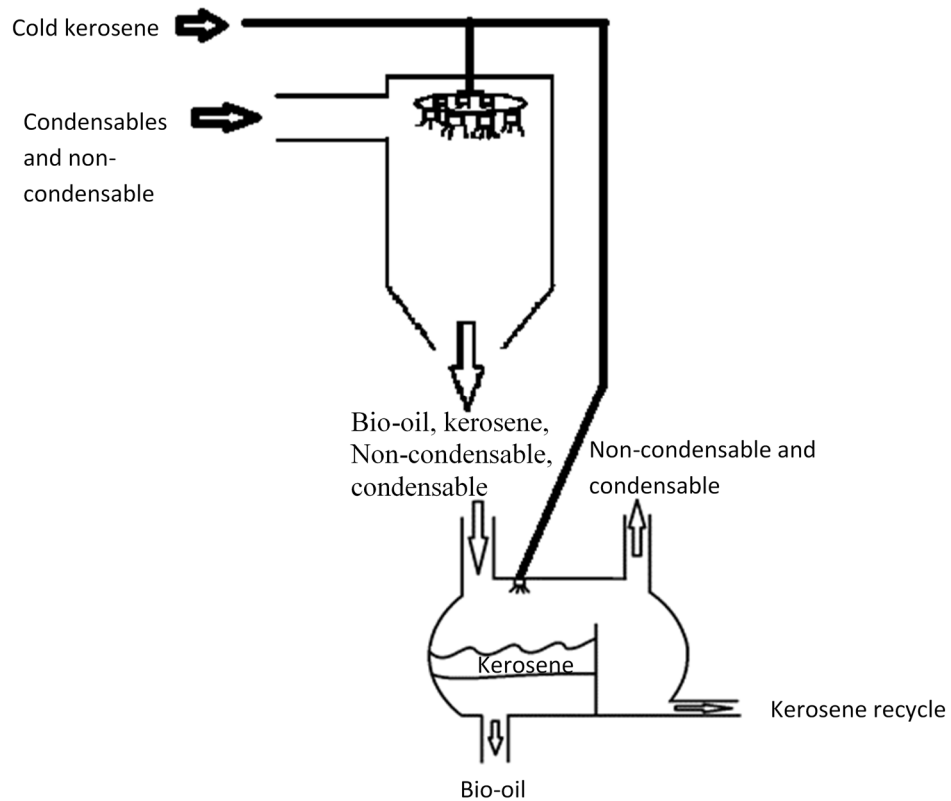


Figure 2. Bio-oil condensing and collection tank diagram.

Figure 3 below shows a block flow diagram of the pilot plant used to produce the bio-oil without the kerosene lines. Figure 2 above is a representation if blocks B3 and B4 below. Tables 2 and 3 summarize the block designations and stream components respectively.

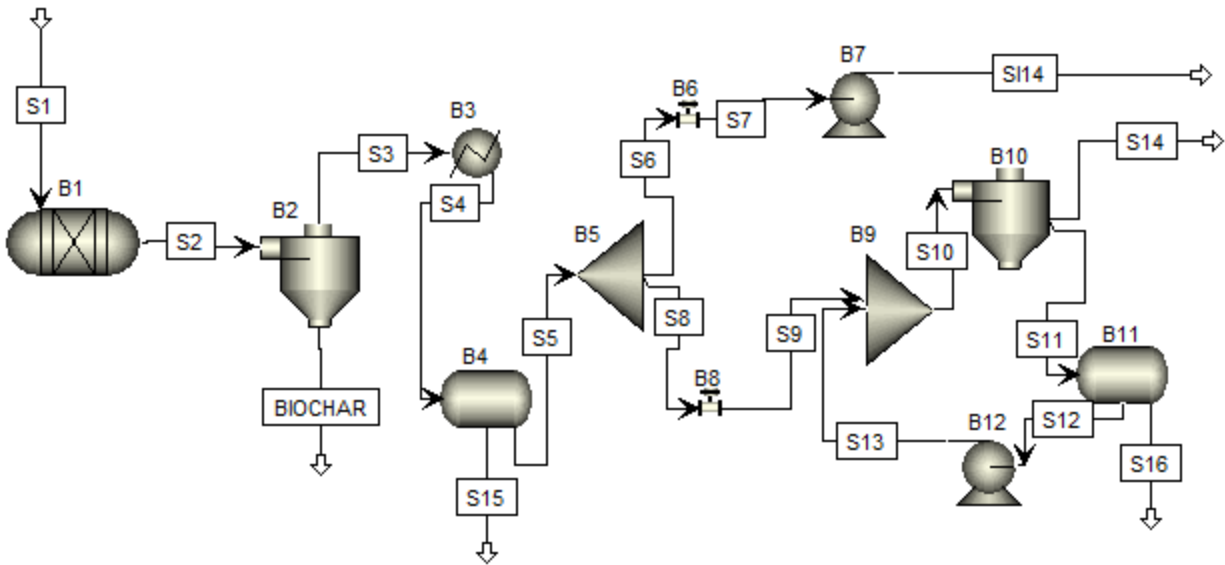


Figure 3. Pilot plant used to make the bio-oil for this research.

Table 2. Pilot plant block designations.

<u>Block</u>	<u>Equipment</u>
B1	Auger reactor
B2	Cyclone
B3	Spray condenser
B4	Vessel
B5	Stream selector
B6,B8	Valve
B7,B12	Pump
B9	Mixer
B10	Cyclone
B11	separating tank

Table 3. Pilot plant stream components.

<u>Stream</u>	<u>Components in stream</u>
S1	dry sawdust
S2	condensable gas, syngas, and bio-char
S3	Condensable gas and syngas
S4	bio-oil, kerosene, condensables and syngas
S15, S16	bio-oil (bottom layer), kerosene (top layer)
S5-S9	syngas and condensables
S10	syngas, bio-oil, and kerosene
S11	Bio-oil and kerosene
S12, S13	Kerosene
S14, S14	Syngas

In the table above, syngas refers to hydrogen, carbon monoxide, carbon dioxide, methane, and other small molecular weight hydrocarbons. Again, there were also trace amounts of bio-char in the bio-oil product. Typical conversions were approximately 56% with continuous runs that pyrolyzed 4 to 15 kg (approximately 8.8-33 lbs.) of sawdust. Piping and vessels were cleaned after each run and new kerosene was occasionally added.

III. Safety, storage, and handling

Due to its low pH and unstable properties, bio-oil has a tendency to corrode most metals so it is usually transported and stored in stainless steel containers (10). HDPE containers may be used as storage containers (23) but it may still be odorous; for this reason, bio-oil was stored in double containers if not under a fume hood. Silver shield gloves, made of polyvinyl alcohol (PVA), were used to handle the bio-oil due to their chemical resistance to many carcinogens and corrosives known to be present in bio-oil. Safety glasses and closed toe leather shoes as well as long pants and other appropriate PPE were worn at all times when dealing with bio-oil, which

was only handled in a fume hood. A lab coat was always worn when working with bio-oil pressurized systems.

IV. Experimental

Two approaches were used in an attempt to remove the water and carboxylic acids: a pressure-driven system and electro-dialysis (ED). The aim of this research was not to synthesize a membrane for the separation but to modify, if needed, commercial membranes to achieve the desired separation. The first step was to find a commercial membrane that was chemically resistant to the corrosive nature of bio-oil. After these modifications were done to the membranes to improve their characteristics, experiments were carried out using bio-oil with ages between a week and 6 months old. The age of the bio-oil is known to affect the water concentration and other properties as well, but since the bio-oil production process conditions were variable, bio-oil samples collected each experiment were used as reference points for experimental sample analysis. Pressure-driven separation experiments were done by placing the membrane in a cell and pressurizing it by closing the exit stream valve, creating a pressure difference on both sides of the membrane since one side of the membrane would remain at atmospheric pressure. This induces permeation through the membrane pores for compounds of the appropriate size if the separating mechanism is size-exclusion.

The ED separation mechanism utilizes charge-induced ion-exchange (IE) membranes. The chemical properties of the membrane allow either anions or cations to transport through the membranes in the presence of an electric field, which drives the separation of the charged species. The anion exchange (AIE) membranes only allow anions through, and the cation-exchange (CIE) membranes, the cations; therefore, the AIE is placed between the oil and the

electrode and the anions from the bio-oil are transported towards the positively charged electrode in an electrolytic solution. The CIE membrane is between the bio-oil and the negatively charged electrode, which is also in an electrolytic solution. It should be noted that there may be hydrogen and chlorine gas formation as a result of an ion species accumulation on a compartment with the electrodes; for the purposes of these experiments, these compartments are referred to as the concentrate compartments. It should also be noted that ED membranes are known to develop material build-up on their surfaces, reversing the electrode polarity every 15 minutes to an hour periodically reduces this effect (30).

A. Membrane modification for pressure-driven separation

Several commercial membranes were tested for material compatibility with bio-oil. Sepro commercial polyamide-piperazine nanofiltration membranes: NF3A, NF3A.1A, XN45, NF2A, and NF6, were tested for compatibility by soaking in bio-oil. Within one hour of the test, all the Sepro membranes had dissolved. Next, a Sterlitech polytetrafluoroethylene (PTFE) laminated membrane with a polypropylene support backing was tested and proved to be chemically resistant; however, the problem with this membrane was that the 50 nm pore size did not allow a separation. The next membrane tested was a sulfonated teflon membrane Nafion 117. This membrane proved to be chemically resistant, but its dense physical characteristics would not allow any permeation of even water alone up to 700 psi. Table 4 below summarizes the membranes tested for bio-oil compatibility and the problems associated with each.

Table 4. Membranes tested for bio-oil compatibility and problems found.

<u>Membrane</u>	<u>Resistant?</u>	<u>Problems</u>
polyamide-piperazine	No	Membranes were dissolved within the hour
Teflon	Yes	Pore size too big, no separation
Nafion	Yes	No membrane permeation

United States patent 6464880 B1 by R. Datta et al. (31) provides a method for the pore expansion of Nafion membranes. This is done by exploding carbon dioxide bubbles on the surface of the membrane. The bubbles are produced by reacting propylene carbonate and water at an elevated temperature; this reaction is summarized below in figure 4.

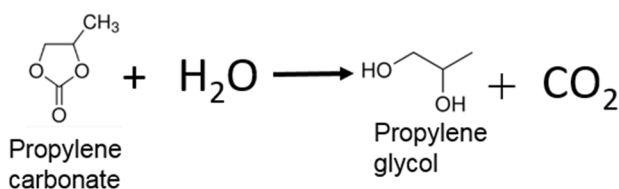


Figure 4 (31). Nafion pore expansion reaction.

In modifying the Nafion membrane, some alterations were made to the process to avoid the use of heat exchangers and sophisticated membrane holders while maintaining the same pre-modification activation steps. The membrane activation was done by first boiling the membrane for 3 hours in DI water, soaking it in a 0.5 N Hydrochloric acid (HCl) solution for 12 hours and soaking it for one hour in DI water. Propylene carbonate (PC) was brought to 100°C in a 2.76 L

Pyrex glass container by means of a hot plate and a stir bar was used for uniform heat distribution. The membrane holder for the modification was a bubble diffuser basket with a lid, both made from a stainless steel sheet which had 1 mm holes approximately 3 mm apart from center to center of the hole. The holder was designed to rest two inches from the bottom of the glass container to clear the stir bar, and steel wire in the shape of handles were tied to the lid. The basket dimensions were 6 in. by 7.75 in. and the lid configured to be slightly smaller to fit inside on top of the membrane to hold it in place. With the exception of the chemicals and membrane, Figure 5 displays the materials used to perform this modification, and figures 6 and 7 display the setup and a close-up of the setup respectively.



Figure 5. Membrane modification materials.



Figure 6. Nafion modification set-up.



Figure 7. Nafion modification set-up close-up.

Propylene carbonate (PC) was heated to 105°C, then the membrane was placed in the membrane holder, and they were placed into the heated PC. Water was then slowly added, bringing the solution to a 6:1 PC to water mole ratio. The liquid level was marked immediately after adding the membrane modification components; the level was monitored and maintained by periodic DI

water addition when needed. A condenser, made from a stainless steel pan with water cooled by means of a chiller or ice, was placed on top of the Pyrex container. A gasket, placed between the Pyrex container and steel pan, was made by sticking the adhesive side of cork material to plexiglass after they were both cut to fit around the edges of the glass container. The cork side of the gasket faced the glass, and the plexiglass made contact with the steel container. A decent seal was achieved with the weight of the water and water only seemed to escape when the temperature was checked by means of a thermocouple. The temperature initially dropped when the water, membrane, and its holder were added to the PC, but it was brought back to 100°C, the optimum reaction temperature, within 10 minutes by slightly adjusting the hot plate setting. The membrane was modified between 4 to 12 hours each run. After the modification was done, the reaction solution and the membrane, removed from the basket, were cooled to room temperature (~23°C) within 10 minutes after the modification. This was done by transferring the reaction solution and the membrane into a steel pan cooled by an ice water bath at which point the membrane was soaked in DI water for 1 hour followed by rinsing, also with DI water.

There was an increase in area after the modification and a slight shrinkage after the last DI water soak; therefore, the membrane was not cut to the size needed until after DI water rinses proceeding the last DI water soak. The temperature was monitored periodically and the hot plate setting was adjusted accordingly to keep the modification solution at 100°C. A few runs were done before familiarity with the hot plate behavior was established; eventually, the runs were done with the temperature ranging from 97°C to 105°C.

B. Pressure-driven experiment procedure

The pressure-driven experiments were performed by using an Osmonics Sepa cell 2 as the membrane cell with Sterlitech Teflon-lined gaskets. Figure 8 below shows a picture of the assembled Sepa cell used for these experiments.



Figure 8. Assembled Osmonics Sepa cell 2.

Each experimental run required 1 liter of bio-oil and the modified Nafion membranes were used with a Teflon membrane for mechanical support. Each experiment was operated at a constant pressure and the pressures tested were 200, 300, 400, 500, 600, and 700 psi. Temperatures of the samples were to be recorded and then subjected to further analysis. Samples were to be collected in a 100ml graduated cylinder for 60 seconds for flux calculations, and 15ml of that were to be transferred into a 15ml sample cuvette and the rest returned to the bio-oil holding vessel. The following procedure was used to set-up the Sepa cell with the cell fitting connections already installed, the Sepa cell manual should be consulted if this is not the case.

Sepa Cell 2 set-up

1. Insert the feed spacer into the center of the cell and the gaskets, if necessary, into the appropriate grooves in the bottom half of the cell.
2. Cut out a membrane whose perimeter fits in between both gaskets which is held by the four small columns (roughly 14 X 19 cm).
3. Place the permeate feed carrier on the center of the top half of the cell and slightly wet with a DI water bottle. (This is done so the permeate feed carrier will stay centered when combining both halves of the cell.)
4. Insert the cell all the way into the cage with the osmonics logo facing the front (the user)
5. Connect the pipes and hoses into the fittings of the connections of the permeate outlet, feed inlet and concentrate outlet streams.
6. Connect the compression pump on the left-hand side of the pump by pressing the pump's brass fitting into the cage connection and press until it locks in place with a click, then turn the outer ring 45 degrees to lock into place.
7. Propel the compression pump until the pressure gauge on the side of the cell cage reads at least 30% higher than the operating pressure.
8. The cell is now ready to use

A hydra cell diaphragm pump with Teflon seals was used to transport the bio-oil to the membrane. It should be noted that with though these pumps are known for their self-priming capabilities, the reduction in head because of the Teflon seals may require priming of the pump

before running an experiment. The pump was primed for each experiment. Stainless steel piping was used to connect the pump to the Sepa cell and a backpressure gauge was placed at the Sepa cell exit stream valve used to control the operating pressure of the cell. A high-density polyethylene (HDPE) bucket was used as the bio-oil vessel and the system was operated at full recycle with the permeation hose also feeding into the bucket. Figure 9 below shows a schematic for the pressure-driven separation set-up as well as the piping material and functional ratings.

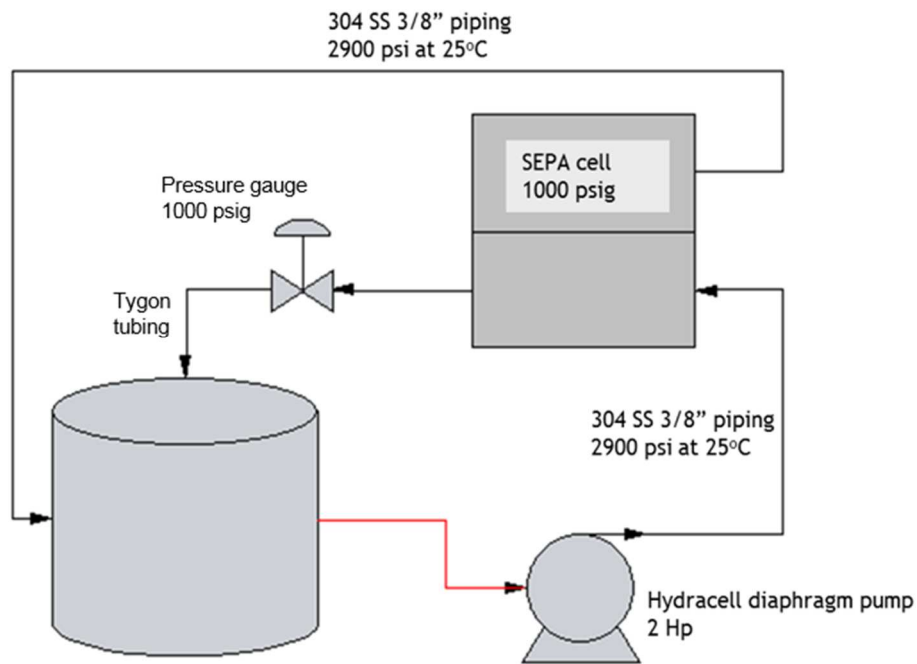


Figure 9. Pressure-driven separation process schematic.

The following procedure was used to set-up the experimental process displayed above in figure 9, and to carry out the runs.

Experimental Set-up/procedure for pressure-driven separation

1. Pump the Sepa cell cage compressing pump to 900 psi.
2. Connect the cooling coil inlet to the appropriate cooling water source and feed the outlet into the appropriate drain.
3. Pour the 1L of the bio-oil or experimental solution into the bucket and, after taking a temperature measurement, close the bucket with its lid and cooling coil.
4. Make sure the concentrate outlet valve is fully open (turning the knob counterclockwise will open it), and that the permeate hose and pump inlet and outlet hoses are fed into the bucket (for total recycle).
5. Connect the pump into the appropriate electrical socket connection, (if not already done so) and press the corresponding ON button.
6. Examine the lines for any leaks, if any, shutoff the apparatus immediately. If none, then close the concentrate outlet valve slowly (turning clockwise) increasing the pressure until the operating pressure is reached. This should take approximately 30 seconds. Inspect the cell during this process, if there are leaks, turn off the pump, disassemble and repeat the SEPA 2 cell set-up procedure making sure the gaskets are uncompromised.
7. If there are no leaks, once the operating pressure is stable, start a stop watch. Then gather samples from the permeate outlet stream with graduated cylinder at time values of 5, 10, 20, 30, and 60 minutes, or as desired.

8. After the experiment is over, allow the excess fluids in the lines to drain into the bucket, then move the lid with the coils and lines to a separate container and dispose of the waste in the appropriate waste container.
9. Open the concentrate outlet valve and add 500ml (or appropriate amount) of DI water and run for 3 minutes to flush the system, twice. Then run again with DI water for second flux calculation to see if irreparable damage is done (flux increases more than ~10%).
10. Disassemble the SEPA 2 cell and dispose or store the membrane properly.
11. Reassemble the Sepa cell and rinse with a 500 ml (or appropriate amount) 40% ethanol solution (or appropriate cleaning solvent) by pumping it through the system then disposing of the solution in to a hazardous waste container by pumping air through the system ONLY IF A HYDRACELL PUMP IS BEING USED, otherwise there may be damages to the pump. Do this three times, then do three rinses the same way with DI water. The rinse solutions should be disposed of properly between each rinse.
12. Disconnect the lines and turn off the cooling water, allowing any excess water to drain by elevating the coil and placing both hoses in the drain.
13. Wash all glassware used by first rinsing with ethanol (or appropriate solvent) and then water. The three-rinse method should be used. Then store everything into its appropriate storage place.

C. Membrane modification for electro-dialysis (ED)

Commercial Anion exchange (AIE) membrane AMX did not seem to dissolve when soaking in bio-oil, but it seemed to develop bio-fouling due to the darkening of its color. Hestekin et al. (32) published an AIE membrane modification procedure for grafting polyethyimine groups onto its surface to reduce membrane bio-fouling. The membrane modification procedure consisted of the three following soaks (32):

1. 1% sodium alginate for 30 minutes
2. 1% polyethylenimine for 60 minutes
3. 2% glutaraldehyde for 60 minutes

The membranes, modified and unmodified, were soaked in bio-oil for 12 hours and a Fourier transform Infrared (FTIR) spectroscopy analysis was performed to test for bio-fouling. The analysis proved the modified membrane to have better resistance to fouling than the unmodified membrane. The FTIR analysis is shown below in figure 10.

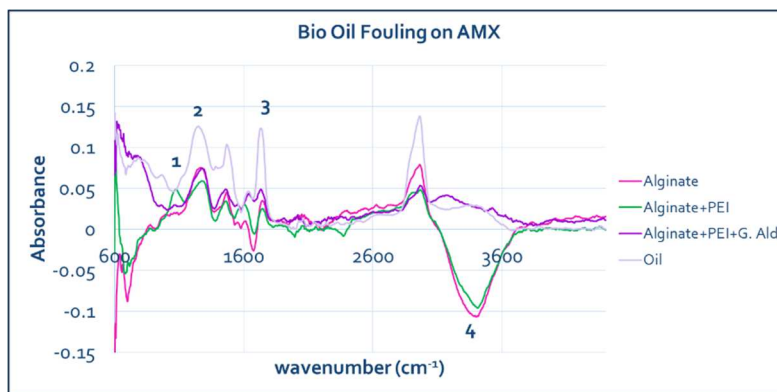


Figure 10. FTIR of Bio-oil soaked membranes.

The figure above shows the absorbance of the bio-oil soaked membranes after each step of the modification soak with the subtraction of the water-soaked membrane samples and the “Oil” line represents the bio-oil soaked unmodified membrane absorbance. The figure above shows larger peaks for the unmodified bio-oil soaked membrane at points 1, 2, and 3, indicating a larger presence of C-O-H at 1050 cm^{-1} , C-O-C at 1200 cm^{-1} , and carbonyl (C=O) at 1700 cm^{-1} respectively, the peaks expected for carboxylic acids. These findings led to the decision to use these membranes, the modified and unmodified, for the electro-dialysis (ED) experiments to determine if the bio-fouling resistance affected its performance, if any, in the carboxylic acid separation.

D. Electro-dialysis procedure

The ED experiments were performed with the three-compartment glass ED. Two 2.0 by 2.5 cm platinum electrodes powered by a Gwinstek GPS-3030DD dc power supply. Unmodified commercial cation exchange (CIE) membranes were used on the side with the negatively charged electrode. The bio-oil was in the middle compartment and a 0.5 M sodium chloride (NaCl) solution was used for the concentrate (outer) compartments.

Glass cell set-up

All experiments were carried out with the glass cell on a glass pan in case of a leak or a spill. Figure 11 below shows the glass cell compartments described in the set-up procedure.

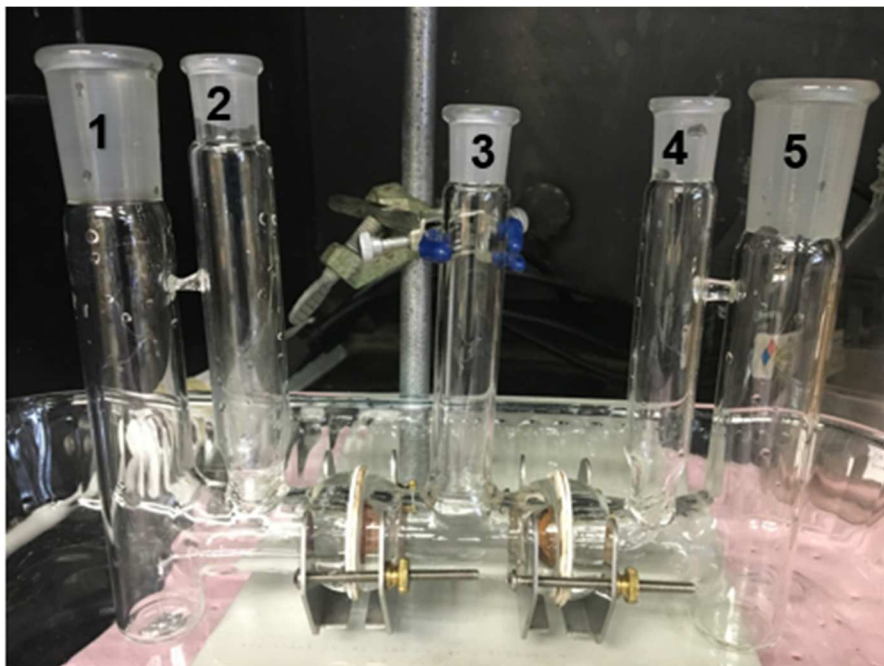


Figure 11. ED glass cell compartments.

Teflon ED gaskets 4.2 cm in diameter were used on both sides of each membrane, which were cut to the same size. The gaskets and membranes were centered as well as possible and the glass cell was kept from leaking by ensuring the metal bracket bottom were parallel to the gaskets, as shown in figure 12 below where the glass cell is seen to be upside down.

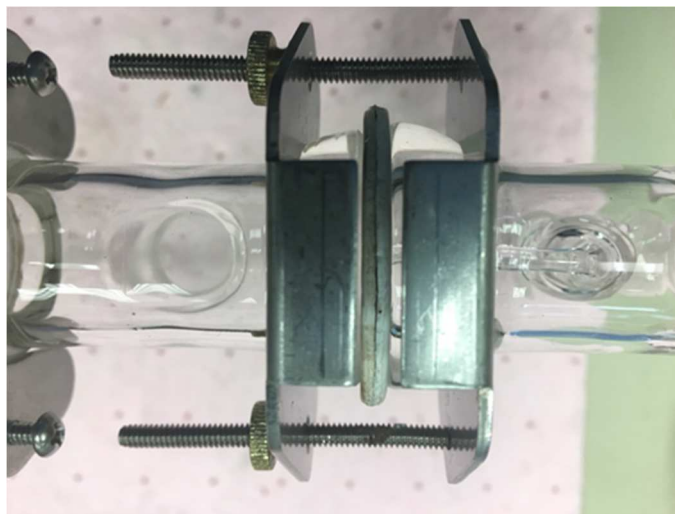


Figure 12. Correct glass cell bracket installed.

The nuts on both sides were simultaneously tightened by hand, with an AIE and CIE membrane placed in between compartments 2 and 3, and compartments 3 and 4 respectively. Rubber stoppers were placed on compartments 2 and 4 to prevent fluid from entering them. The two concentrate compartments, 1 and 5, were filled with approximately 65 mL of a 0.5 NaCl solution and an electrode was placed on each side. Para-film was wrapped around the glass openings of the electrode holders and the two electrodes were made to face each other. Approximately 45 mL of bio-oil was poured into compartment 3 and para-film was used to seal the top of that compartment. Then the power source was connected to the electrodes as shown in figure #13; the positively charged electrode was connected to the side contacting the AIE membrane, compartment 1 and the negatively charged electrode was placed on the compartment that was in contact with CIE membrane, compartment 5. Figure 13 below shows the ED glass cell set-up and ready for experimentation.

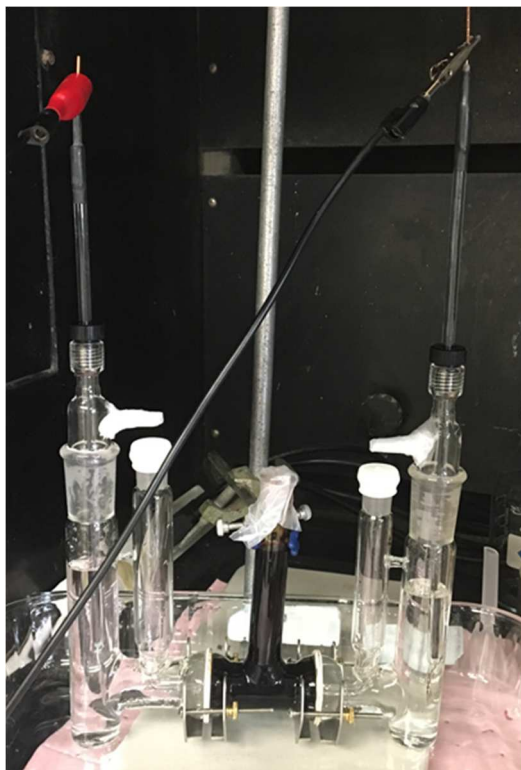


Figure 13. ED glass cell set-up.

ED experimental procedure

The power source was turned on with the constant voltage of 5V and varying current. Current and conductivity were monitored with time and samples were taken periodically from compartments 1, 3, and 5. The compartments were filled as needed and experimental runs were carried on for 24 to 109 hours. After every use, the glass cell was cleaned with acetone and water, then washed with soap and water.

V. Analysis

No samples were taken from the pressure-driven separation experiments system runs due to a lack of permeation. The Nafion 117 membranes were modified up to 12 hours and though there was a considerable change in area, as a result of pore expansion, bio-oil would not permeate through the membrane at pressures up to 700 psi. Membranes were run for a minimum of an hour under pressure before discontinuing the experiment. The pore size of the 12-hour modified Nafion membrane was analyzed for pore size.

ED experimental samples were taken from the bio-oil and two concentrate compartments and were then analyzed for water concentration, the bio-oil and acidic species composition, the concentrate compartment samples. The membranes were also analyzed with regard to bio-fouling and separation performance. Table 5 below summarizes the labels given to the experiments done.

Table 5. ED summary of experiments.

<u>Experiment</u>	<u>membrane type</u>	<u>refills(hr.)</u>	<u>Concentrate solution</u>
P1	Modified	6	0.5M NaCl
P3	Unmodified	6,24	0.5M NaCl
P5	Modified	3,22(C)/22(B)	0.5M NaCl
P7	Unmodified	7.5, 26 (C)/26(B)	0.5M NaCl
P15	Modified	3,22(C)/22(B)	0.5M NaCl

Experiments that used bio-oil from the same batch were P1 and P3, as well as P5 and P7.

Experiment P15 used bio-oil from a different batch. Differences in bio-oil initial conductivity

values may be due to a lack of thorough homogenization before experimentation. The refills column in the table above states the hour of the experiment at which the compartments were filled. The (C) next to the refill hour on some entries signifies the refilling of the concentrate compartments, the (B) stands for the bio-oil compartment. ED concentrate compartment samples were analyzed by HPLC using a Waters IC-Ion Exclusion column with a refractive index detector. The samples were tested for formic, acetic, propionic, and butyric acids but the retention times did not match those from the samples. These results may be found in Appendix D. Approximately 4 months after the samples were taken, the concentrate compartment samples were observed through a microscope to test the orange color for salt precipitates.

A. Membrane pore size analysis

Jamie et al. (33) reported that modifications on the Nafion 112 membrane gave nanofiltration pore size membranes, for this modified set-up, modification time deviations were expected. Though a separation was not achieved for the pressure-driven experiments, the pore size distribution of membranes tested is important for future bio-oil experiments with porous membranes. Evaporimetry (EP) was used to determine the pore size distribution (PSD) of the modified membranes from the vapor pressure depression that occurs for a volatile wetting liquid in small pores. Since vapor pressure depression increases as the pore diameter decreases, evaporation of the volatile wetting liquid with uniform saturation over its surface will progress in time from the largest pores to the smaller ones (34). By means of a gravimetric analysis and the help of the Kelvin equation, rates of evaporation can be related to pore diameters, which can be used to determine the PSD of a membrane. Takei et al. (35) showed the Kelvin equation to be accurate down to 4 nm pores and the equations used for the analysis may be found in Appendix C.

Method

FTIR scans were taken of the modified Nafion membrane and compared to the unmodified one to confirm the change the membrane experienced was strictly physical. For the EP analysis, the membrane was placed in a holding cell with a round opening where the membrane is exposed and where it is also filled with the wetting fluid, in this case, isopropyl alcohol (IPA). A Mettler Toledo MS104S micro balance was tared with the membrane holder and membrane in place. At that point, the sample cell was filled with IPA and the initial weight and decreasing weights, due to evaporation, were automatically recorded every 5 seconds. A small beaker with activated carbon was also placed nearby the cell in case of contaminants and though the balance had a stock casing to isolate the balance, a cardboard box was set in place to minimize any effects the balance may feel from the air flow of in the room. Figure 14 below shows a picture of the membrane sample cell used in the EP analysis and figure 15 shows the balance set-up with the membrane cell and activated carbon.



Figure 14. EP membrane sample holding cell.



Figure 15. EP set-up with the scale, membrane sample cell, and activated carbon.

Results

Figure 16 below shows the FTIR scans taken for a commercial unmodified membrane and a 4-hour modified membrane.

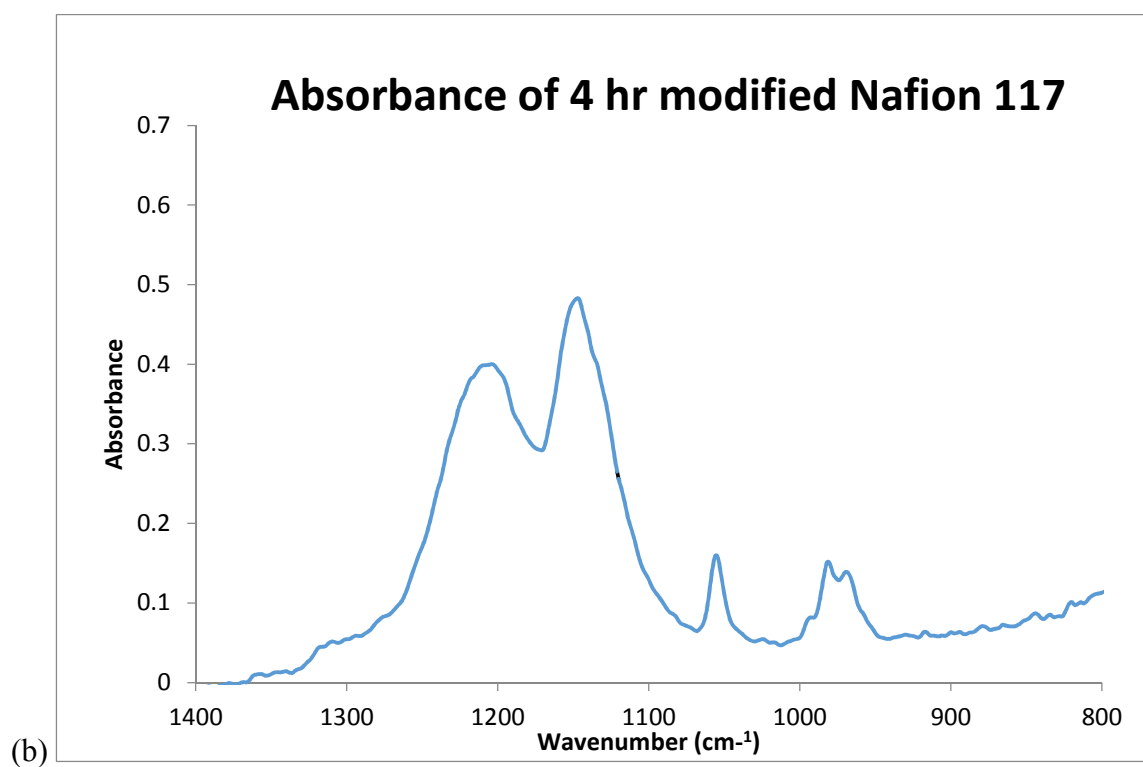
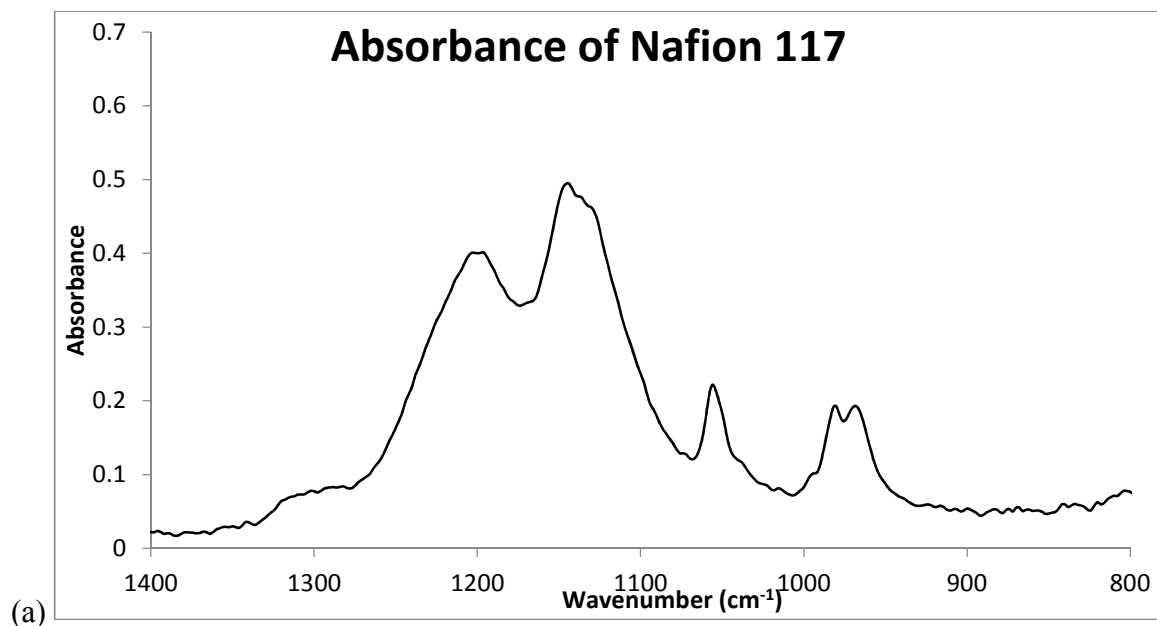
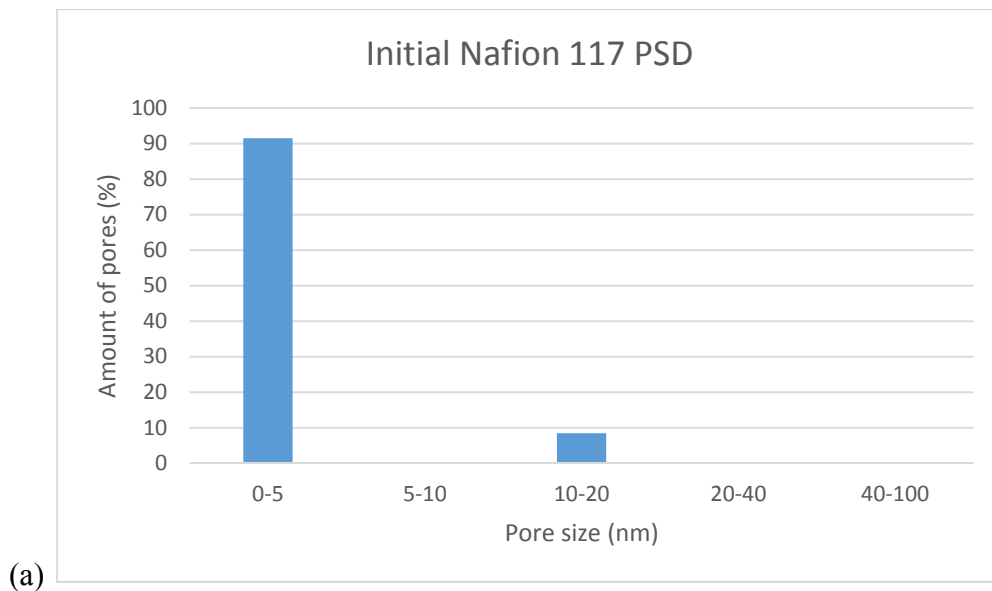


Figure 16. FTIR Absorbances for (a) commercial Nafion 117 and (b) 4-hour modified Nafion 117.

The two Absorbance graphs above are identical, confirming the reaction does not compromise the chemical nature of the membrane. The modified Nafion membranes experienced an increase in size with the pore expansion modification. A membrane with an initial size of 12 by 17 cm expanded to approximately 14 by 20 cm after a 6-hour modification; however, the membrane was difficult to measure due to the wrinkles that resulted from the modification. Evaporimetry of the Nafion membranes also proved the pore expansion procedure to be successful; this is seen in figure 17 below exhibiting the PSD for the initial and modified Nafion membranes.



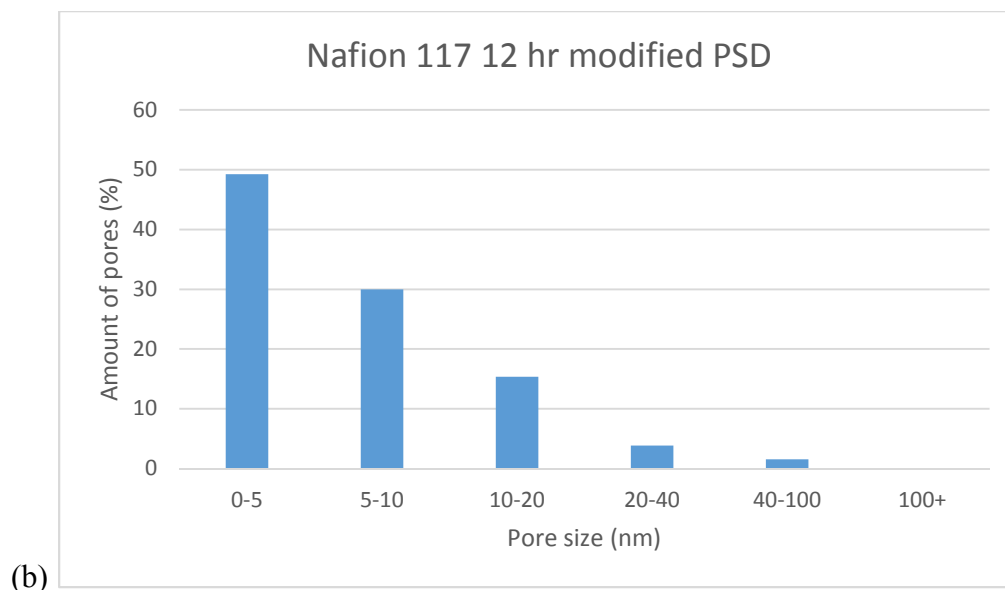


Figure 17. Pore size distribution for (a) Commercial Nafion 117 and (b) 12-hour modified Nafion 117 membrane.

B. Water concentration determination

Water concentration in bio-oil is an important factor when considering using it for fuel. A volumetric Karl Fischer titration for water determination has been suggested by several literature sources (23, 36, 37); unfortunately, very little information of analysis parameters was found with the exception of the type of titrant and solvent used for the analysis. Boucher et al. (36) determined the water concentration in bio-oil by using a Hydranal composite 5 reagent and a 50/50 dichloromethane solvent. Oasmaa et al. (23) used a solvent of 3:1 methanol to chloroform and a KF reagent containing 2-methoxy ethanol with reactive components of the anion of the alkyl sulphurous acid, iodine and base. They claimed that the endpoint was easier to detect when chloroform was present. Mohammed et al. (37) used the CombiSolvent Keto and CombiTitrant 5 Keto as the solvent and titrant respectively, and also used a sodium hydroxide (NaOH) buffer solution to control the pH. The bio-oil water determinations follow the general procedure

presented by ASTM E 203-01 (38). ASTM E 203-01 states that certain precautions need to be taken in determining the water concentrations of acidic and aldehyde and ketone containing samples. Ketones and aldehydes tend to form acetals and ketals with methanol which yield water as a reaction product, giving false measurements of water in the samples (23,39), and acidic samples lower the pH value of the solvent below the optimum pH range of 5 to 8 for accurate water determination (37, 39). Bio-oil is known to fit into both categories. Hydranal K reagents for aldehydes and ketones may be used as a solution for the aldehyde and ketone problem, and an imidazole buffer is recommended to maintain the appropriate pH of the titration of acidic samples (39). It should be noted that methanol free solvents are required for Hydranal K reagents (40).

Method

Water determination for sample analysis was done by using a Mettler Toledo DL31 Karl Fischer volumetric titrator. Aquastar Combititrant 5 Keto and Hydranal Working medium K were used as the reagent and solvent respectively. The parameters had to be adjusted to achieve lower titration times and accurate results; the parameters are summarized below in table 6.

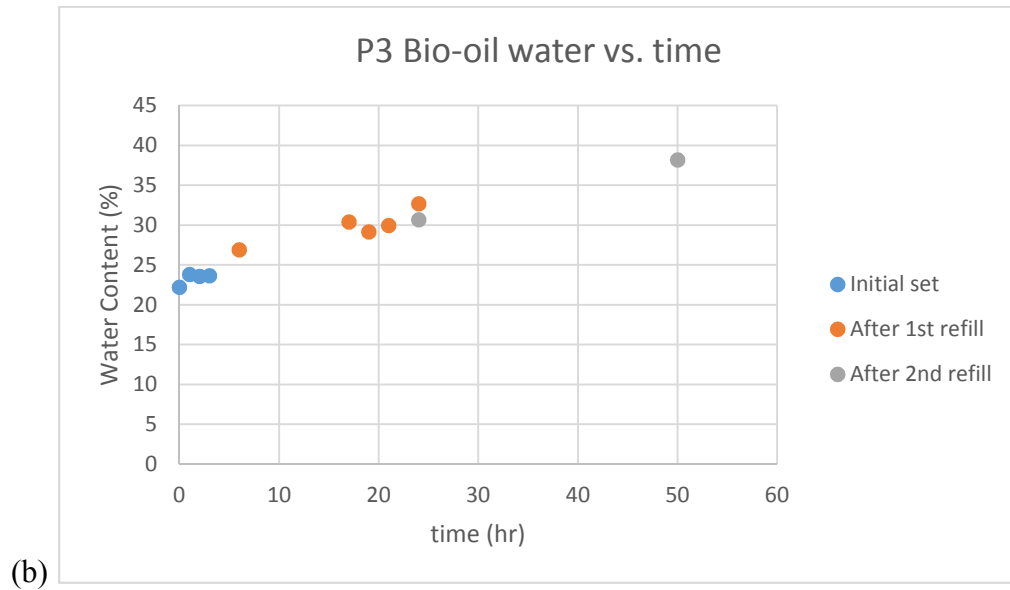
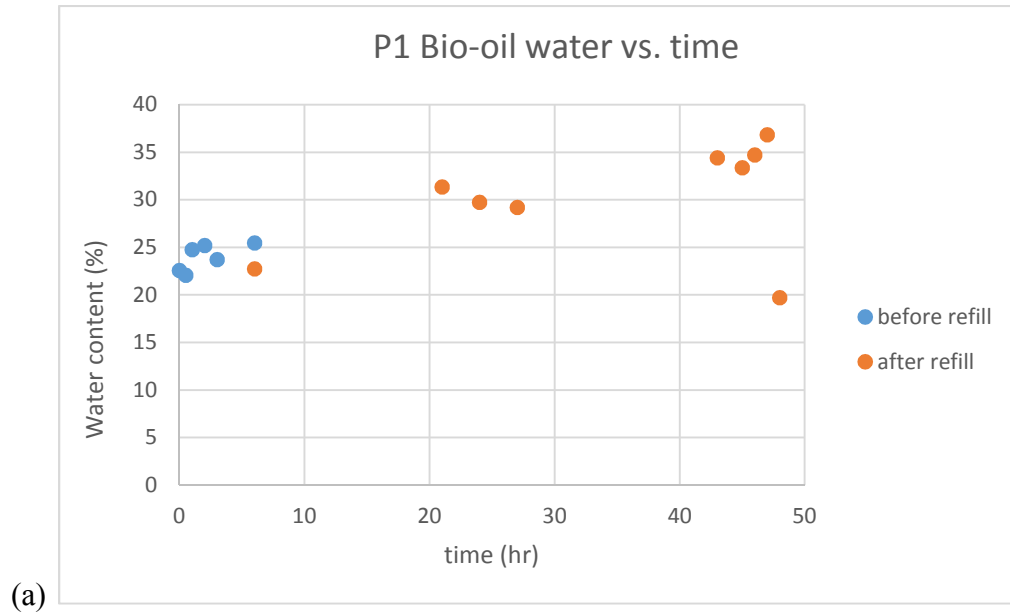
Table 6. DL31 Karl Fischer titration parameters.

Parameter	Value
I _{pol} (μV)	20
E.P. (mV)	175
Stir speed (%)	30-35
ΔV _{min} (μL)	0.5
ΔV _{max} (μL)	4
Rel. Drift (mg/min)	50

In the table above, I_{pol} is the polarization current; E.P. is the end point titration; and ΔV_{min} and ΔV_{max} are the minimum and maximum limits of titrant that may be added at a time. For more information on the DL31 Karl Fischer titrator or how the parameters work, a standard operating procedure (SOP) on it may be found in Appendix E. These parameter values gave average approximate titration times of 2 minutes 20 seconds, but titration times sometimes went as high as 5 minutes. Pre-titration times were anywhere from less than a minute up to 10 minutes. The accuracy of the bio-oil sample results was verified using Hydranal Water Standard 10.0 samples in between bio-oil samples to see if the standard result was accurate, with an error of less than 5% being accepted before the titration solvent was replaced. Experimentation showed that the titration solvent was acceptable for up to 5 bio-oil samples.

Results

Results for the Karl Fischer analysis are summarized below in figure 18.



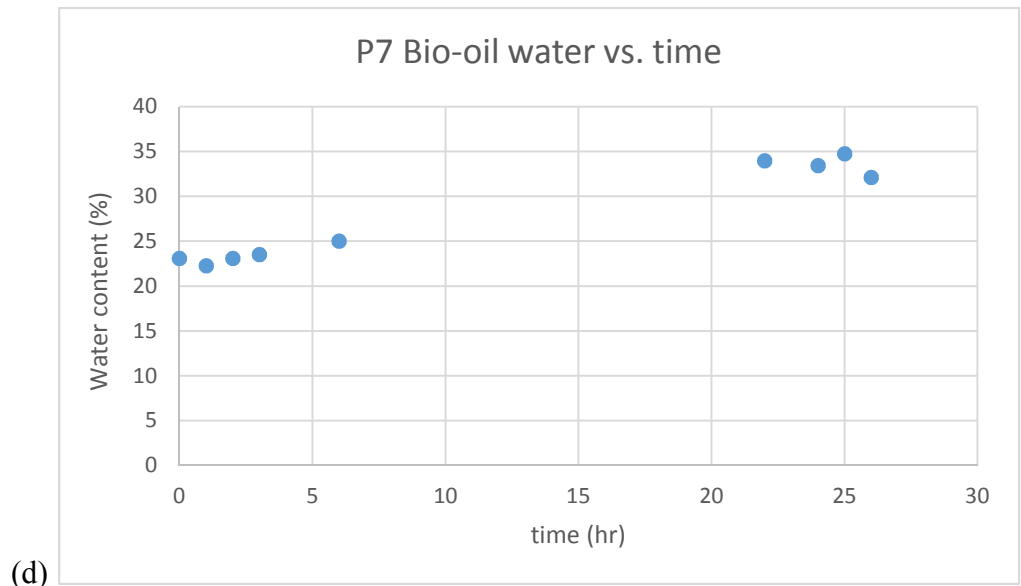
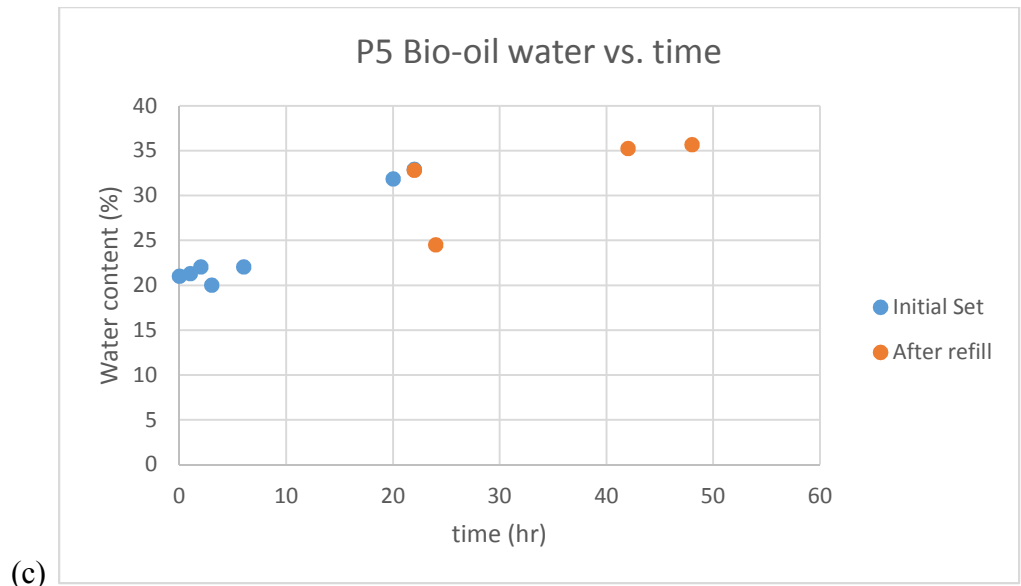


Figure 18. Karl Fischer analysis of Bio-oil ED runs (a) P1, (b) P3, (c) P5, (d) P7.

Water concentration increased for all experiments and reached 38%. Each sample was analyzed twice and analysis results can be found in tabular form for each run in Appendix A.

C. Conductivity and pH

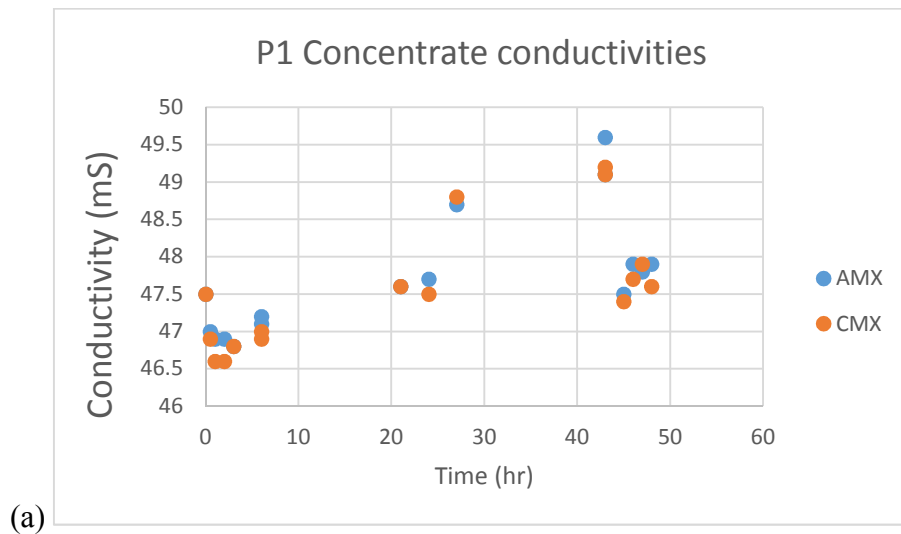
Bio-oil is known to have carboxylic acids and a considerable amount of water. Measuring conductivities and pH's of the compartments is a simple way of noting changes in acidic species. Water concentration affects the dissociation of the acids and, consequently, also the conductivity of the sample being measured.

Method

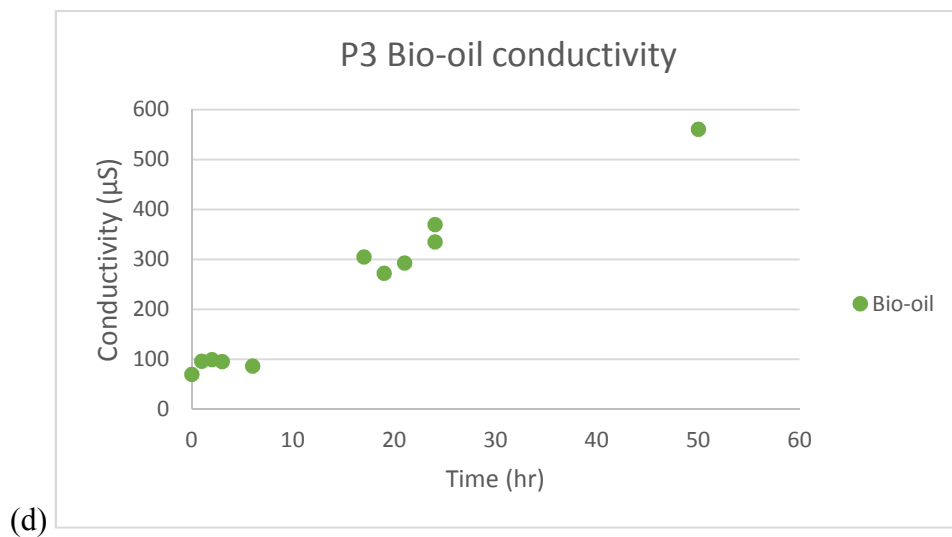
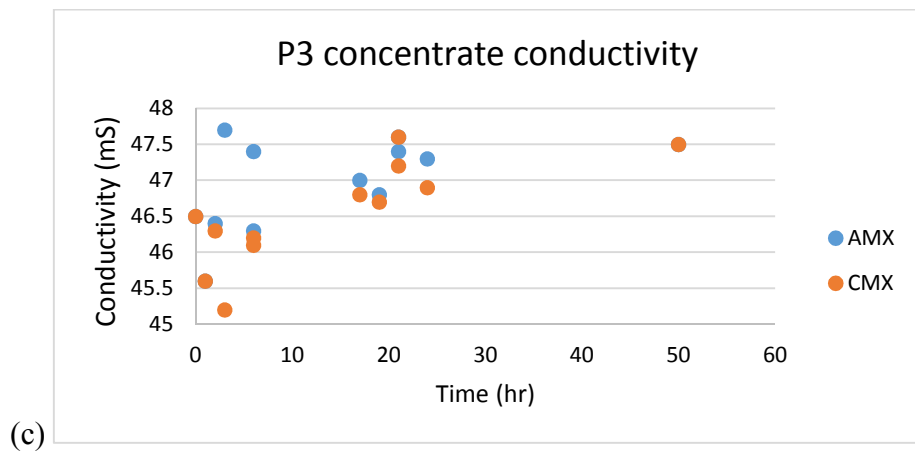
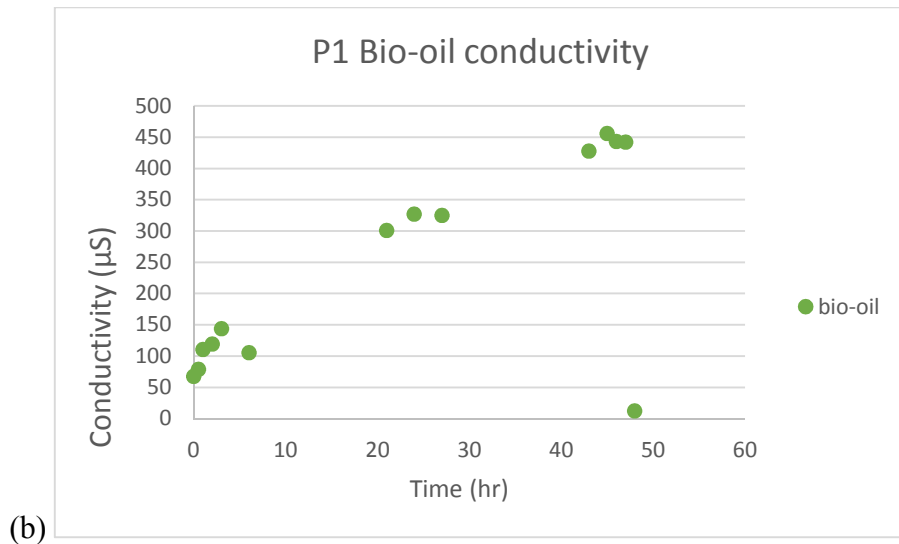
A VWR Traceable conductivity meter was calibrated and used to take the conductivity measurements of the bio-oil and the two concentrate compartments. An Orion model 330 pH meter with an Ag/AgCl Orion 9156DJWP pH probe was used to measure the pH of the concentrate samples.

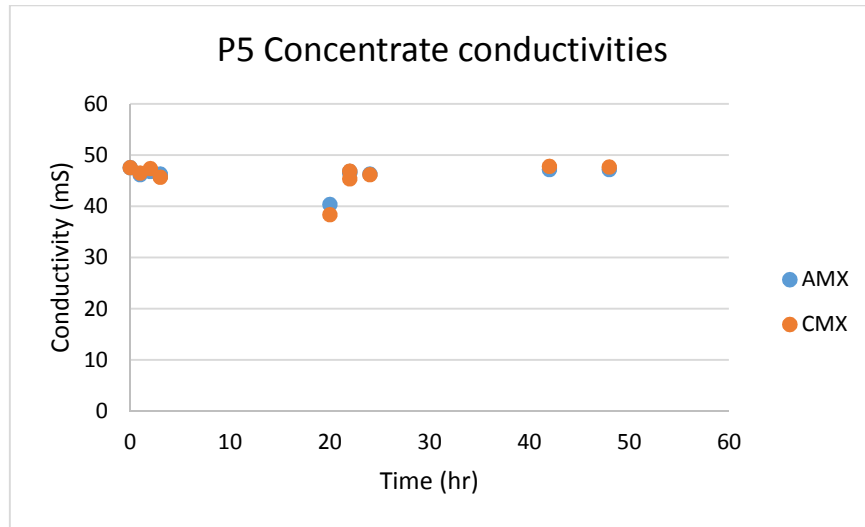
Results

Conductivities of the concentrate and bio-oil compartments are summarized below in figure 19.

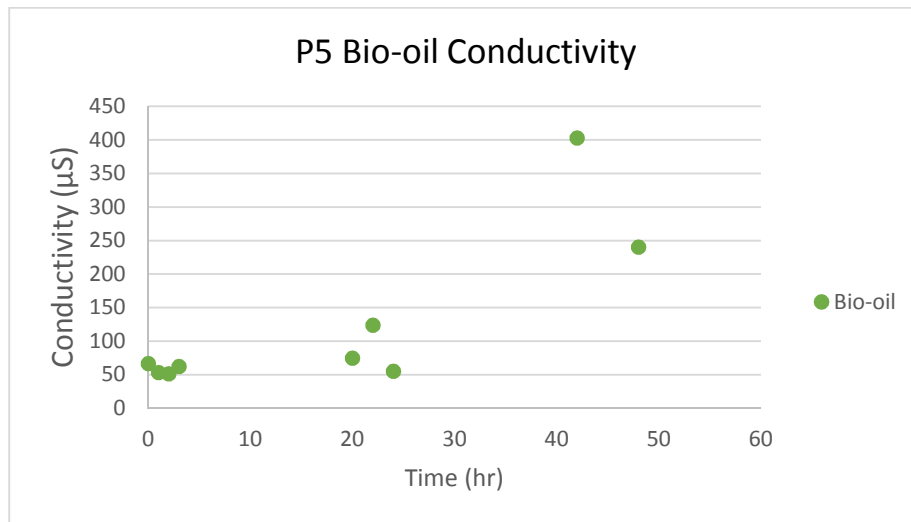


(a)

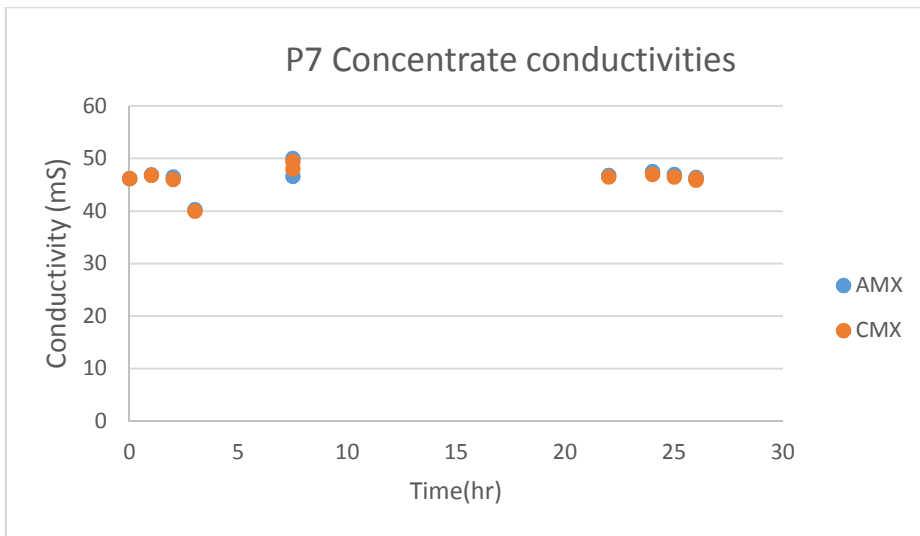




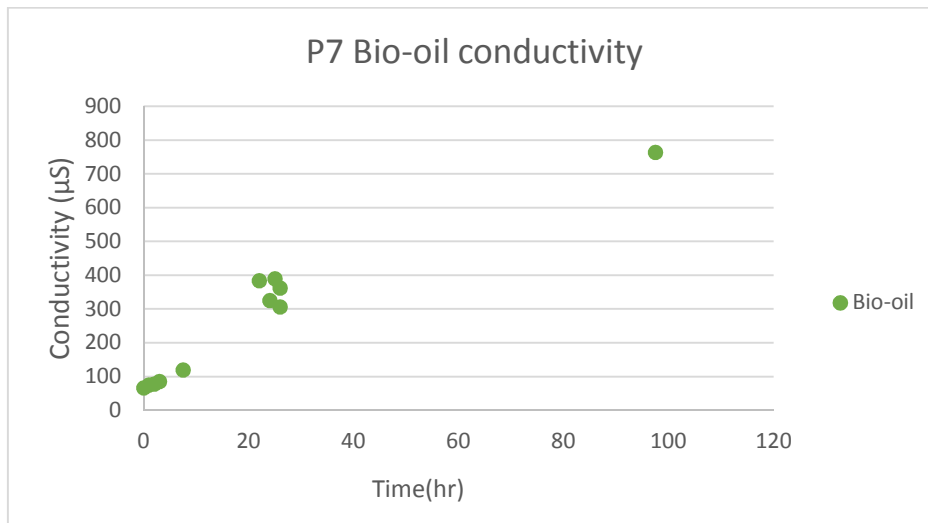
(e)



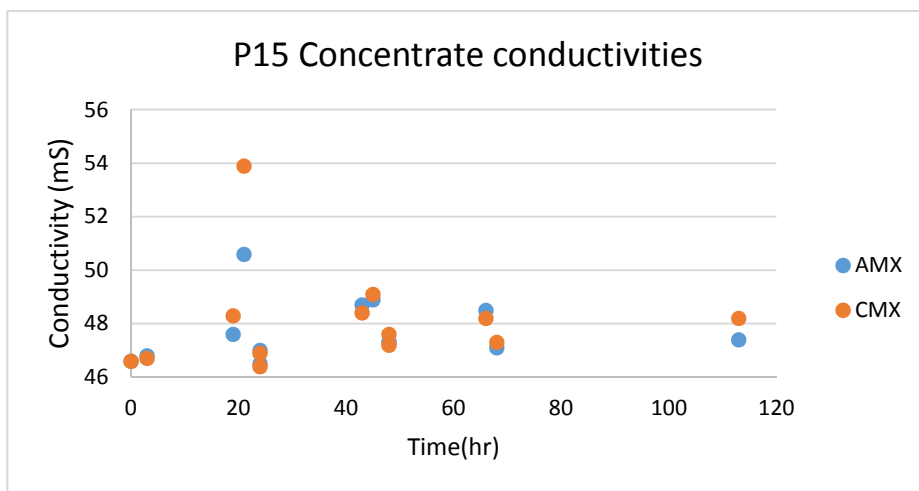
(f)



(g)



(h)



(i)

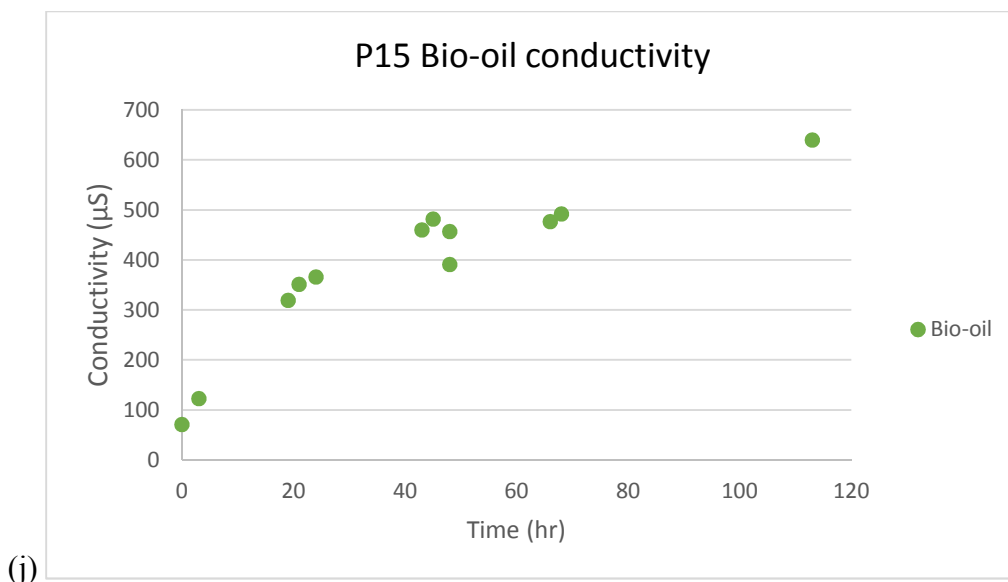
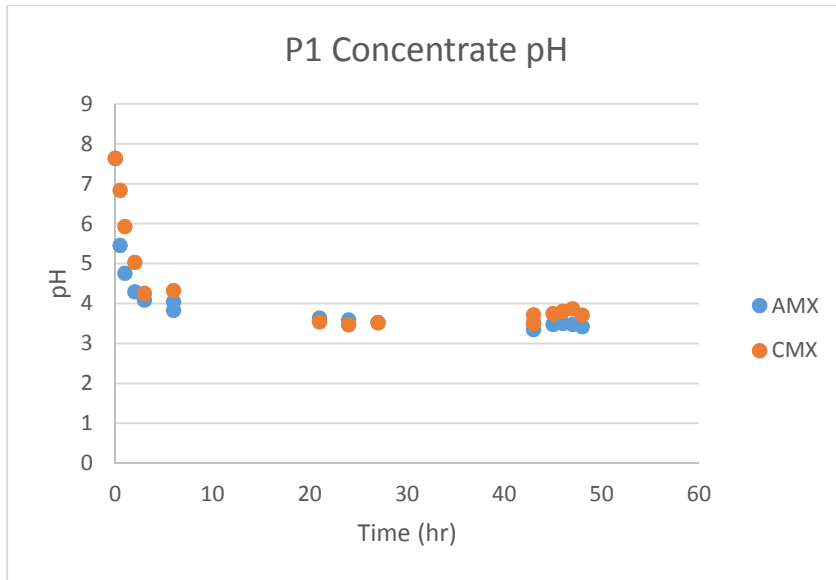
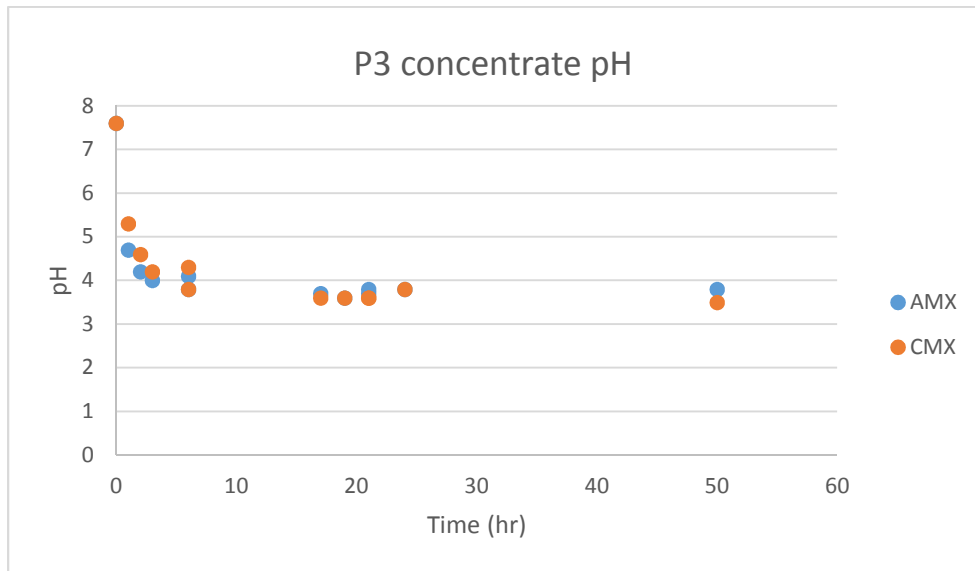


Figure 19. Conductivities of each experiment concentrate compartment and their corresponding bio-oil compartments.

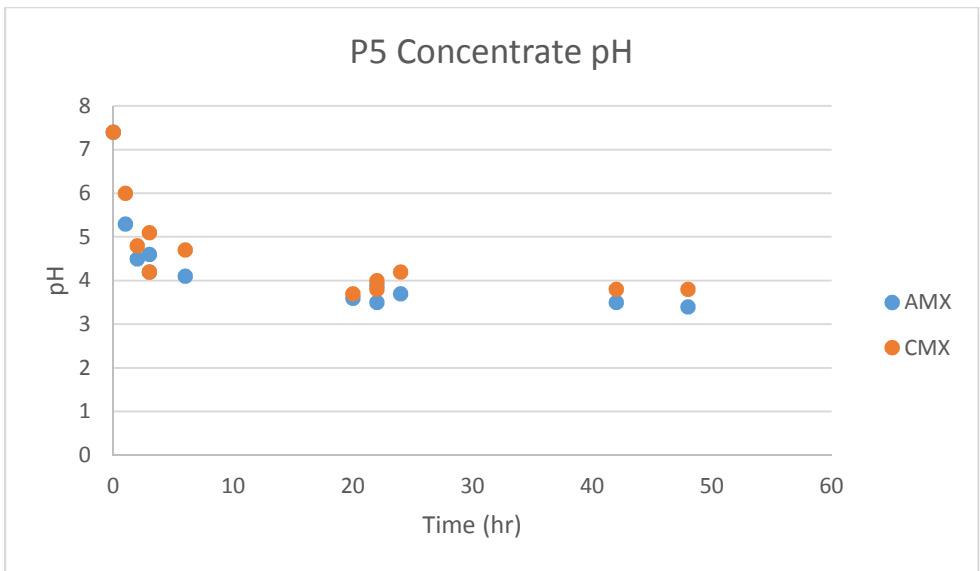
As can be seen in Figure 19, the concentrate samples for P5 and P7 remained relatively linear throughout the experiments and P1 and P3 seem to show a resemblance. For all experiments, the concentrate conductivities remained between 40-50 mS, with the exception of a few outlier points. Bio-oil conductivities for all experiments increased overall, whether the modified or unmodified AIE membrane was used. This increase may be attributed to the increase of the water content in the bio-oil, allowing more dissociation of the acidic species to occur and remain in the bio-oil compartment due to potential concentrate acid saturation or a clogged membrane. Figure 20 below shows the pH of the concentrate compartments throughout the experiment.



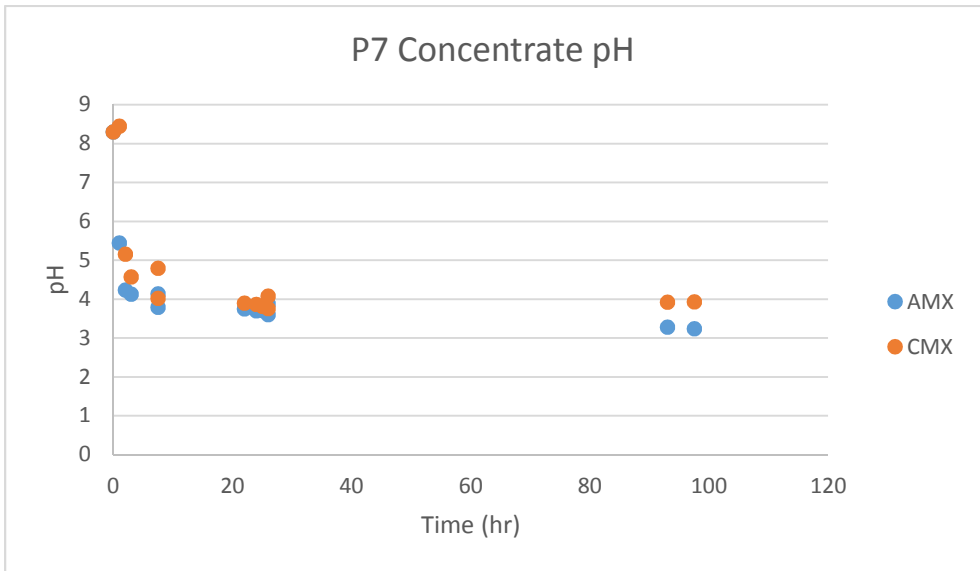
(a)



(b)



(c)



(d)

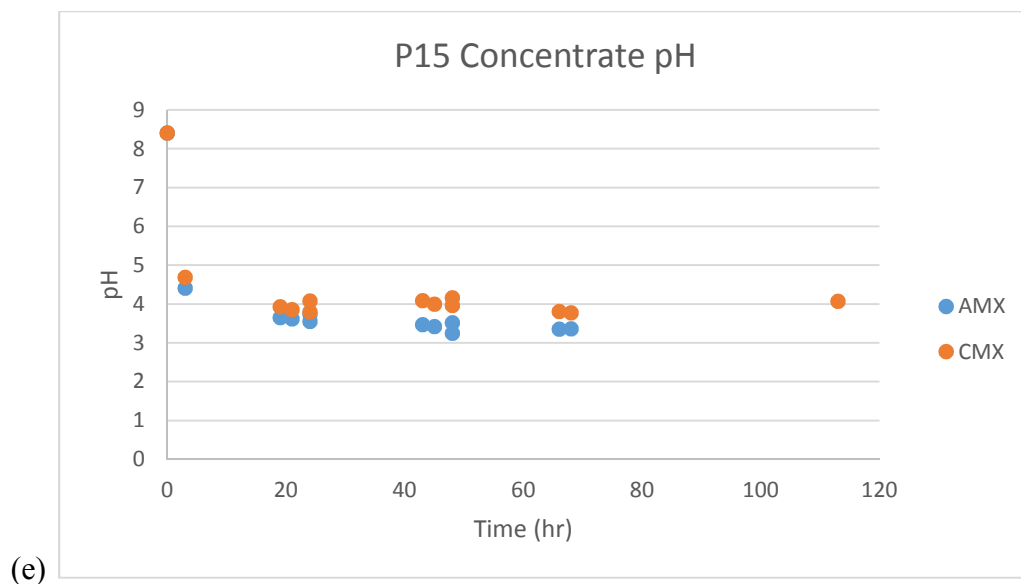


Figure 20. Concentrate sample pH measurements for experiments (a) P1, (b) P3, (c) P5, (d) P7, (e) P15.

The pH measurements appear to be more consistent from run to run, with both concentrate compartments reaching a pH between 3 and 4. Also, in all the experiments but one, P3, the AMX compartment samples were measured to be slightly more acidic than the CMX samples. No significant difference in concentrate compartment pH seems to take place in relation to the membrane used.

D. Membrane surface characterization

Commercial Neosepta AIE AMX and CIE CMX commercial membranes were used for these experiments. Composition information of commercial ion exchange (IE) membranes is limited in literature, but Lin et al. (30) has published, in U.S. patent 8969424 B2, various chemicals that could be used to synthesize these membranes. Lin also stated that having a tertiary amine group with a quaternizing chemical an AIE membrane was found to produce a membrane with good chemical resistance. Although the exact composition of the membranes was not found, there

were general compounds listed as components of the membranes; this is important to analyzing the membranes for bio-fouling to see what components were already there and which ones were a result of the experiment. Poly(vinyl chloride) is reported to be used as the support layer for the ion exchange membranes (41, 42), and the CIE Neosepta CMX membrane is reported to contain a 45-65% sulfonated styrene-divinylbenzene randomly cross-linked copolymer and 45-55% of polyvinylchloride (PVC) manufactured by the paste method. The commercial AIE Neosepta AMX membranes are also reported to be made of the same styrene-divinylbenzene polymer and filler PVC as the CMX membranes (41).

Method

The modified anion membrane was analyzed in several ways. First, a XPS analysis of a modified AMX membrane soaked in bio-oil for one week was compared to that a modified membrane soaked in water. This was done to note the change of the membrane surface when exposed to bio-oil.

Results

For the modified membrane comparison of the one soaked in bio-oil to the one soaked in water, afterward the membranes were rinsed with water and stored in a 0.5M NaCl solution for approximately 3 days. The membranes were thoroughly washed with DI water 24 hours before the analysis and then dried by means of a dessicant. Table 7 summarizes the elemental composition for both membranes: the AMX-M bio which was soaked in bio-oil, and the AMX-M which was the control membrane soaked in water.

Table 7. AMX-M surface elemental composition.

<u>Elements</u>	<u>AMX-M (%)</u>	<u>AMX-M Bio (%)</u>
C (1s)	87.59	92.62
N (1s)	5.86	2.33
O (1s)	4.05	2.87
S (2p)	0.2	0
Si (2p)	0.72	0.71
Cl (2p)	1.58	1.47
total (%)	100	100

The AMX-M membranes compositions were measured after one minute of 2 keV argon sputtering. Elemental peak shifts for carbon are seen in figures 21-23.

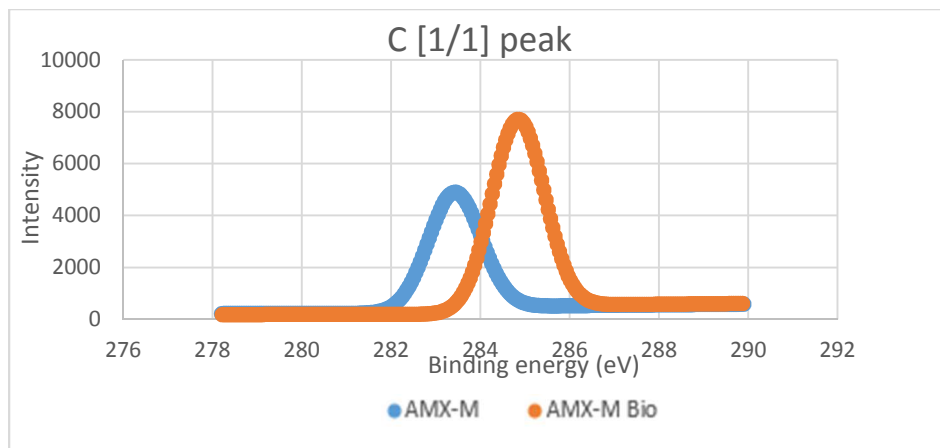


Figure 21. Carbon 1s [1/1] peak shift.

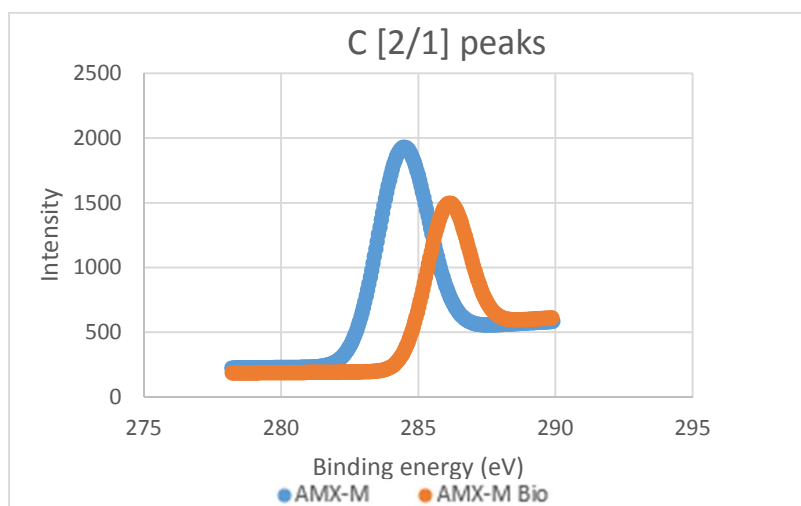


Figure 22. Carbon 1s [2/1] peak shift.

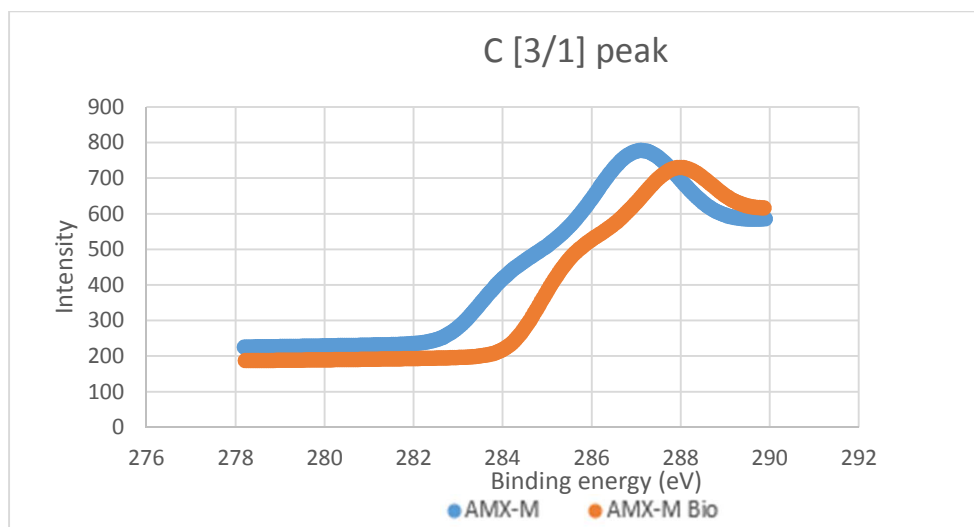


Figure 23. Carbon 1s [3/1] peak shift.

From the figures above, peak [1/1] seems to shift approximately 1.3 eV and the increased intensity points to an increased presence of hydrocarbon hydrogens, which are known to have a binding energy around 284.8 (43). The fact that the binding energies of the carbon peaks shifted to a higher binding energy after being soaked in bio-oil indicates the presence of a more electron withdrawing, oxidative, environment. Extended delocalized electrons in a sample results in low intensity peaks at higher binding energies (44), which is the case for peaks [2/1] and [3/1]. The increase of the carbon is also supported by the oxygen peaks shown in figure 24, and the nitrogen peaks shown in figures 25 and 26 shown below.

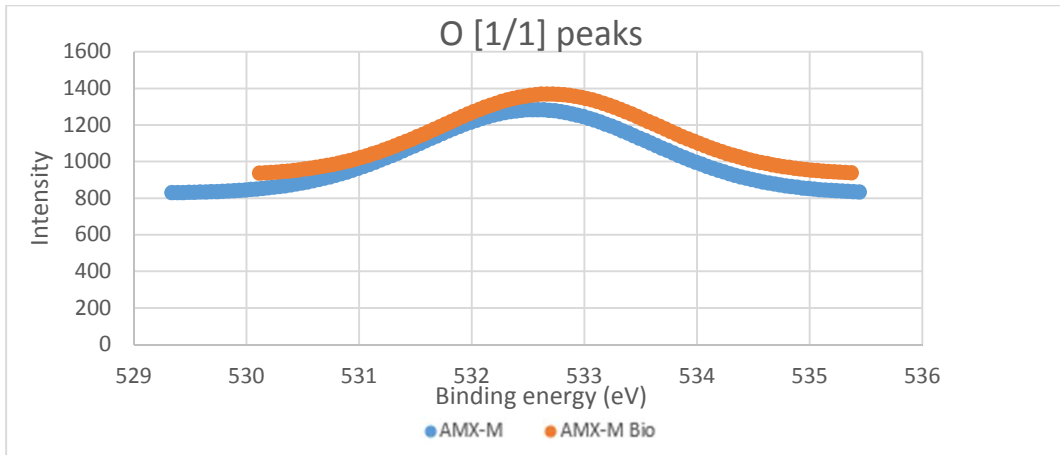


Figure 24. Oxygen 1s peak shift.

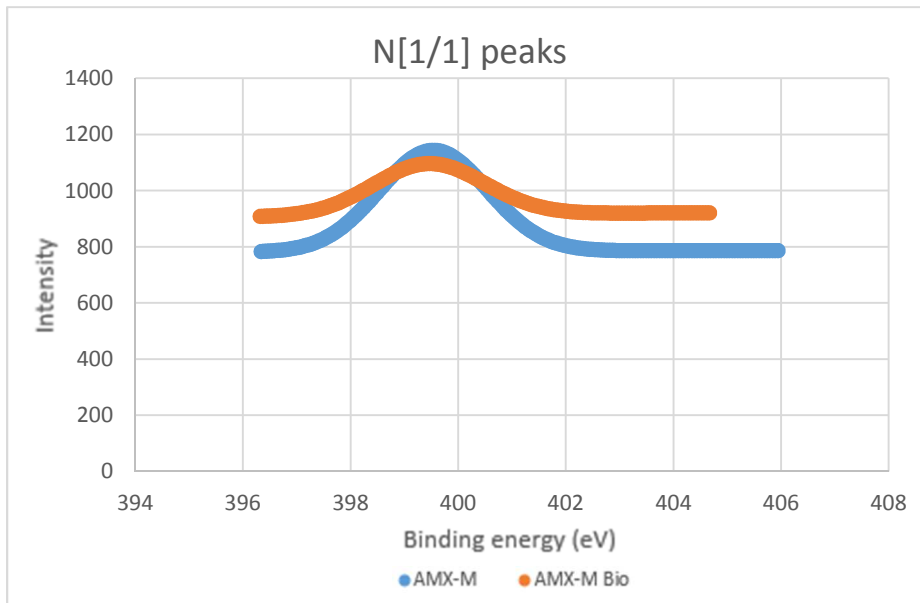


Figure 25. Nitrogen 1s [1/1] peak shift.

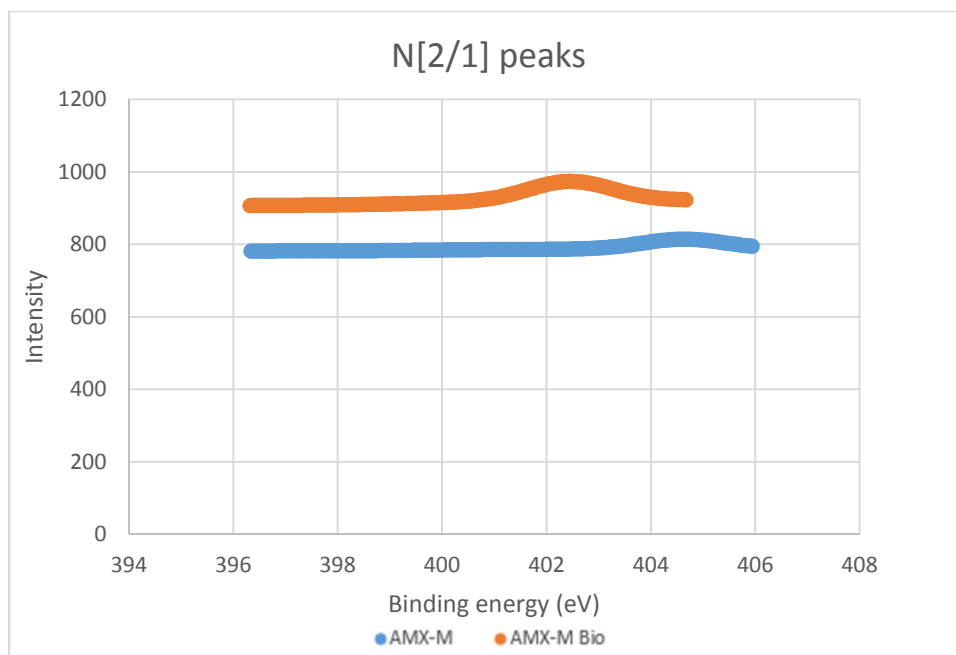


Figure 26. Nitrogen 1s [2/1] peak shift.

The slight oxygen binding energy decrease of the bio-oil soaked membrane is due to the increased electron donating carbon content. The same is the case for the nitrogen [2/2] peak, and the lower intensity of nitrogen is due to the layer of carbon on the surface of the membrane from the bio-oil. Sulfur peaks were only found on the controlled membrane, reinforcing the fact that there was significant build-up on the surface of the membrane due to the bio-oil.

VI. Conclusion

Though the Nafion pore expansion was successful, the membrane with the Teflon-lined polypropylene support proved to be ineffective at removing the water from bio-oil. Future work in this area should incorporate the use of other hydrophilic membranes, such as MEEK or PVDF membranes, for Nafion support. Longer modification times may be appropriate but a careful

balance should be kept since the mechanical strength of the Nafion membrane decreases with the increase of modification time.

Electrodialysis was successful in removing a portion of the acidic species from the bio-oil but not the water. Although the modified AMX membrane proved to experience less bio-fouling than the unmodified commercial membrane, it still experienced some. Future work in this area should include either more hydrophobic membranes to keep the water the same, or membrane modifications, if not synthesis, to remove water with the carboxylic acids as well.

IX. Literature Cited

1. **Zhou, R., et al.**, "Effects of Reaction Temperature, Time and Particle Size on Switchgrass Microwave Pyrolysis and Reaction Kinetics," *International Journal of Agricultural and Biological Engineering* **6** (1), pp. 53-61 (2013).
2. **Basu, P.**, "Pyrolysis," Chapter 5, "Biomass Gasification, Pyrolysis and Torrefaction Practical Design and Theory," 2nd ed., Elsevier, Saint Louis, MO, (2013).
3. **Mohan, D., et al.**, "Pyrolysis of Wood/Biomass for Bio-oil: A Critical Review." *Energy & Fuels*, **20** (3), pp. 848-889 (2006).
4. **U.S. Environmental Protection Agency**, "Criteria Air Pollutants," <https://www.epa.gov/criteria-air-pollutants>, EPA, (Aug. 2016).
5. **U.S. Department of Agriculture**, "Major Uses of Land in the United States, 2007," Economic Information Bulletin No. 89, USDA, (Dec. 2011).
6. **Farag, I. H., et al.**, "Technical, Environmental and Economic Feasibility of Bio-Oil in New Hampshire's North Country Final Report to the New Hampshire Industrial Research Center (NHIRC)," Project No. 14B316 UDKEIF, www.unh.edu/p2/biooil/bounhif.pdf, Chemical Engineering Department of the University of New Hampshire, (2012).
7. **U.S. Department of Agriculture**, "Pyrolysis Oil-Overview of Characterization and Utilization," Publication No. 256524, Agricultural Research Service, (2011).
8. **Chiaramonti, D., et al.**, "Power Generation Using Fast Pyrolysis Liquids from Biomass," *Renewable and Sustainable Energy Reviews*, **11** (6), pp. 1056-1086 (2007).
9. **Pakdel, H., and C. Roy**, "Production and Characterization of Carboxylic Acids from Wood Part I: Low Molecular Weight Carboxylic Acids," *Biomass*, **13** (3), pp. 155-171 (1987).
10. **U. S. Department of Agriculture and County Governments cooperating**, "Pyrolysis and Bio-oil," Cooperative Extension Service Report FSA1052-PD-6-09N, Fayetteville, AR (2009).

11. **Zhu, X., and Q. Lu**, "Production of Chemicals from Selective Fast Pyrolysis of Biomass," Chapter 8 in Momba, M., and F. Bux, eds., "Biomass," pp. 147-164 (2010).
12. **Piskorz, J., et al.**, "Pretreatment of wood and cellulose for production of sugars by fast pyrolysis," *Journal of Analytical and Applied Pyrolysis*, **16**, pp. 127-142 (1989).
13. **Shen, D.K., et al.**, "Study on the Pyrolytic Behaviour of Xylan-based Hemicellulose Using TG-FTIR and Py-GC-FTIR," *Journal of Analytical and Applied Pyrolysis*, **87** (2), pp. 199-206 (2010).
14. **Yaman, S.**, "Pyrolysis of Biomass to Produce Fuels and Chemical Feedstocks," *Energy Conversion and Management*, **45** (5), pp. 651-671 (2004).
15. **Spearpoint, M. J., and J.G. Quintiere**, "Predicting the Burning of Wood Using an Integral Model," *Combustion and Flame*, **123** (3), pp. 308-325 (2000).
16. **Liden, A.G., et al.**, "A Kinetic Model for the Production of Liquids from the Flash Pyrolysis of Biomass," *Chemical Engineering Communications*, **65** (1), pp. 207-221 (1988).
17. **Caprariis, B. D., et al.**, "Kinetic Analysis of Biomass Pyrolysis Using a Double Distributed Activation Energy Model," *Journal of Thermal Analysis and Calorimetry*, pp. 1403-410 (2015).
18. **Sharma, A., et al.**, "Biomass pyrolysis-A review of modeling, process parameters and catalytic studies," *Renewable and Sustainable Energy Reviews*, **50**, pp. 1081-1096 (2015).
19. **Zhang, J. et al.**, "Multi-Gaussian-DAEM-reaction Model for Thermal Decompositions of Cellulose, Hemicellulose and Lignin: Comparison of N₂ and CO₂ Atmosphere," *Bioresource Technology*, pp. 87-95 (2014).
20. **Shen, D.K., and S. Gu**, "The Mechanism for Thermal Decomposition of Cellulose and Its Main Products," *Bioresource Technology*, **100** (24), pp. 6496-6504 (2009).

21. **Boutin, O., et al.**, "Radiant Flash Pyrolysis of Cellulose—Evidence for the Formation of Short Life Time Intermediate Liquid Species," *Journal of Analytical and Applied Pyrolysis*, **47** (1), pp. 13-31 (1998).
22. **Oasmaa, A., et al.**, "Acidity of Biomass Fast Pyrolysis Bio-oils," *Energy & Fuels Energy Fuels*, **24** (12), pp. 6548-6554 (2010).
23. **Oasmaa, A., and C. Peacocke**, "Properties and Fuel Use of Biomass derived Fast Pyrolysis Liquids: A Guide," *VTT Publications*, **731** (79), (2010).
24. **U.S. Department of Energy**, "A review of the Chemical and Physical Mechanisms of the Storage Stability of Fast Pyrolysis Bio-Oil," Publication No. NREL/SR-570-27613, DOE National Renewable Energy Laboratory, Golden, CO (Jan. 2000).
25. **Naranjo, S., et al.**, "Compatibility of Fast Pyrolysis Bio-Oil/Bioethanol Blends with Plastic Polymers," Proceedings of the 13th International Conference on Environmental Science and Technology, Athens, Greece (Sept. 5-7, 2013).
26. **Kirk, D. W., et al.**, "Materials compatibility with Pyrolysis Biofuel," Proceedings of ASME Turbo Expo 2001, New Orleans, LA (June 4–7, 2001).
27. **Fuleki, D.**, "Bio-fuel System Material Testing," *PyNE Newsletter*, (7), pp. 5-6 (Apr. 1999).
28. **Soltes, E. J., and S. K. Lin**, "Hydroprocessing of Biomass Tars for Liquid Engine Fuels," In: Tillman, D. A. & Jahn, E. C. (eds.). *Progress in Biomass Conversion*. New York: Academic Press, pp. 1–69. (1984).
29. **ASTM International**, "Standard Specification for Pyrolysis Liquid Biofuel," Designation D7544-12, ASTM, (2012).
30. **Lin, J. R., and J. Lin**, "Anion Exchange Membranes and Process for Making," United States Patent Patent No. US 8969424 B2, (Mar.24, 2013).

31. **Datta, R. et al.**, "Microporous Ionomeric Materials and Methods of Preparation," United States Patent No. US 6464880 B1, (Oct. 15, 2002).
32. **Hestekin, J., et al.**, "Electrochemical Enhancement of Glucose Oxidase Kinetics: Gluconic Acid Production with Anion Exchange Membrane Reactor," *Journal of Applied Electrochemistry*, pp. 1049-1052 (2002).
33. **Hestekin, J., et al.**, "Modified Porous Nafion®: Membrane Characterization and Two-phase Separations☆," *Journal of Membrane Science*, **281**, pp. 268-273 (2006).
34. **Akhondi, E., et al.**, "Evaporimetry Determination of Pore-size Distribution and Pore Fouling of Hollow Fiber Membranes," *Journal of Membrane Science*, **470**, pp. 334-345 (2014).
35. **Takei, T., et al.**, "Validity of the Kelvin Equation in Estimation of Small Pore Size by Nitrogen Adsorption," *Colloid & Polymer Science*, **275** (12), pp. 1156-1161 (1997).
36. **Boucher, M.E., et al.**, "Bio-oils Obtained by Vacuum Pyrolysis of Softwood Bark as a Liquid Fuel for Gas Turbines. Part I: Properties of Bio-oil and Its Blends with Methanol and a Pyrolytic Aqueous Phase," *Biomass and Bioenergy*, **19** (5), pp. 337-350 (2000).
37. **Mohammed, I. Y., et al.**, "Novel Method for the Determination of Water Content and Higher Heating Value of Pyrolysis Oil," *BioResources*, **10** (2), (2015).
38. **ASTM International**, "Standard Test Method for Water Using Volumetric Karl Fischer Titration," Designation E 203-01, ASTM, (2001).
39. **Mettler Toledo**, "Mettler Toledo DL31/DL38 Titrators Applications brochure 26,".
40. **Scholz, E.**, "Organic Compounds," "HYDRANAL-Manual" Riedel-de Haën, Seelze, Germany, p. 57 (2012).
41. **Pismenskaya, N. D., et al.**, "Evolution with Time of Hydrophobicity and Microrelief of a Cation-Exchange Membrane Surface and Its Impact on Overlimiting Mass Transfer," *Journal of Physical Chemistry B*, **116** (7), pp. 2145-2161 (2012).

42. **Yamane, R., et al.**, "Studies on Ion Exchange Membranes. XXI. Preparation of SO_4^{2-} Non-permselective Anion Exchange Membranes," *Journal of the Electrochemical Society of Japan*, **32** (3), pp.134-142 (1964).
43. **Tang, C.Y., et al.**, "Effect of Membrane Chemistry and Coating Layer on Physiochemical Properties of Thin Film Composite Polyamide RO and NF Membranes: I. FTIR and XPS Characterization of Polyamide and Coating Layer Chemistry," *Desalination*, **242** (1), pp. 149-167 (2009).
44. *XPS Reference: Table of Elements*, Thermo Fisher Scientific Inc., Web, (Oct. 26, 2016) <http://xpssimplified.com/periodictable.php>, (2016).
45. **Krantz, W. B., et al.**, "Evaporometry: A Novel Technique for Determining the Pore-size Distribution of Membranes," *Journal of Membrane Science*, **438**, pp. 153-166 (2013).

X. Appendix

A. Karl Fischer Raw data

Table A1. P1 KF results

	Time (hrs.)	Sample 1	Sample 2	Average
	0	22.6891	22.4677	22.5784
	0.5	22.0135	22.1409	22.0772
	1	24.8027	24.714	24.75835
	2	25.2324	25.1483	25.19035
	3	23.8243	23.6153	23.7198
	6	25.2896	25.6104	25.45
refill	6	22.059	23.419	22.739
	21	30.785	31.9528	31.3689
	24	29.2395	30.2065	29.723
	27	29.1787	29.208	29.19335
	43	34.5834	34.2522	34.4178
	45	33.6061	33.1114	33.35875
	46	34.8079	34.6	34.70395
	47	36.3792	37.32	36.8496
	48	19.8021	19.6086	19.70535

Table A2. P3 KF results

	Time	Sample 1	Sample 2	Average
	0	22.3319	22.0505	22.1912
	1	23.8237	23.743	23.78335
	2	23.4808	23.6342	23.5575
	3	24.0983	23.1729	23.6356
R	6	26.6423	27.1349	26.8886
	17	30.91	29.8655	30.38775
	19	29.1678	29.096	29.1319
	21	29.5174	30.3763	29.94685
	24	32.1077	33.2672	32.68745
R	24	30.8786	30.4605	30.66955
	50	38.107	38.2591	38.18305

Table A3. P5 KF results

Time (hr.)	Sample 1	Sample 2	Average
0	21.5133	20.5252	21.01925
1	21.235	21.3996	21.3173
2	22.5304	21.5818	22.0561
3	20.8325	19.2297	20.0311
6	22.3789	21.7104	22.04465
20	31.258	32.4832	31.8706
22	32.2844	33.6052	32.9448
22	33.6806	32.003	32.8418
24	25.6654	23.3952	24.5303
42	35.2534	35.2928	35.2731
48	36.0325	35.3323	35.6824

Table A4. P7 KF results

Time (hr.)	Sample 1	Sample 2	Average
0	23.6027	22.5606	23.08165
1	22.2519	22.2582	22.25505
2	23.5946	22.553	23.0738
3	23.1923	23.8325	23.5124
6	25.8572	24.1813	25.01925
22	33.5011	34.4342	33.96765
24	34.548	32.3519	33.44995
25	33.7458	35.7715	34.75865
26	30.7671	33.4718	32.11945

B. Evaporometry equations

These are the equations used for the determination of the membrane pore distribution published by Krantz et al. (45). This analysis assumes a round pore surface and that the molar flux is small; these assumptions were justified in the published work and were shown to contribute up to 1% to the measured pore diameter error. Table B1 shown below defines the equation parameters.

Table B1 (45). Equation parameters

d	pore diameter (nm)
d_c	Cell diameter (cm)
γ	surface tension (g/s ²)
V_A	liquid molar volume of liquid A (cm ³ /mol)
T	Temperature (K)
k_x^o	gas-phase mass transfer coefficient (mol/cm ² s)
k_x	mass transfer coefficient at small fluxes (mol/cm ² s)
x_{A0}	gas-phase mole fraction of A at membrane surface
x_{A0}^o	gas-phase mole fraction of A at liquid layer surface
J_S^*	gas-phase molar flux of A with respect to the molar-average velocity (mol/cm ² s)
N_A	molar flux of A with respect to a stationary reference frame (mol/cm ² s)
W_A	evaporation rate of liquid A during pore draining (mol/s)
W_A^o	evaporation rate of liquid A overlying the membrane (mol/s)
π	pi
R	Universal gas constant

The following form of the Kelvin equation was used to determine the membrane pore diameter:

$$d = -\frac{4\gamma V_A}{RT \ln(x_{A0}/x_{A0}^o)} \quad (1)$$

Mass transfer k_x^o with respect to the molar average velocity is described by the following equation

$$k_x^o = \frac{J_S^*}{x_{A0}} = \frac{N_A(1-x_{A0})}{x_{A0}} = \frac{4W_A(1-x_{A0})}{\pi d_c^2 x_{A0}} \quad (2)$$

The mass transfer coefficient is related to the mass transfer coefficient with small mass transfer flux by the following film theory equation:

$$k_x = -\frac{x_{A0}k_x^o}{(1-x_{A0})\ln(1-x_{A0})} \quad (3)$$

Combining equations (2) and (3) the following equation is obtained:

$$k_x = -\frac{4W_A}{\pi d_c^2 \ln(1-x_{A0})} \quad (4)$$

Rearranging equation (4) and solving for

$$x_{A0} = 1 - e^{-(4W_A/\pi d_c^2 k_x)} \quad (5)$$

$$\begin{aligned} \frac{x_{A0}}{x_{A0}^o} &= \frac{1 - e^{-(4W_A/\pi d_c^2 k_x)}}{1 - e^{-(4W_A^o/\pi d_c^2 k_x)}} \cong \frac{-(4W_A/\pi d_c^2 k_x) + \frac{1}{2}(4W_A/\pi d_c^2 k_x)^2 - \dots}{-(4W_A^o/\pi d_c^2 k_x) + \frac{1}{2}(4W_A^o/\pi d_c^2 k_x)^2 - \dots} \quad (6) \\ &\cong \frac{W_A}{W_A^o} \end{aligned}$$

This approximation by using the Taylor series allows the measurable rate of evaporation to be related to pore diameter.

C. Bio-oil GC/MS

Table C1. Distillate Organic phase

RT	MW	compound	Area	% total
4.886	92.14	toluene	1.78E+07	0.3
6.972	116.16	4-hydroxy-4-methyl-2-pentanone	4.39E+07	0.6
7.885	106.16	p-xylene	5.77E+07	0.8
8.615	106.16	o-xylene	3.07E+07	0.4
8.821	128.2	nonane	6.71E+07	0.9
9.919	142.28	3-methyl nonane	3.32E+07	0.5
10.1	142.28	3-ethyl-2-methyl heptane	2.70E+07	0.4
10.78	140.27	2,6-dimethyl octene	3.68E+07	0.5
10.84	128.26	3-ethyl heptane	4.33E+07	0.6
10.88	120.19	1-ethyl-2-methyl benzene	5.98E+07	0.8
10.95	142.28	2-methyl nonane	9.26E+07	1.3
11.16	120.19	trimethyl benzene	1.09E+08	1.5
11.98	120.2	trimethyl benzene	1.88E+08	2.6
12.14	142.28	decane	3.94E+08	5.5
12.83	184.36	trimethyl decane	2.05E+08	2.9
14.06	156.31	4-methyl decane	1.56E+08	2.2
14.2	156.31	2-methyl decane	1.10E+08	1.5
15.35	156.31	undecane	6.89E+08	9.7
16.96	134.22	1,2,3,4-tetramethylbenzene	1.29E+08	1.8
17	170.33	2,6-dimethyl decane	9.22E+07	1.3
17.29	170.34	2-methyl undecane	2.09E+08	2.9
18.14	138.16	2-methoxy-4-methyl phenol	1.15E+08	1.6
18.37	170.33	dodecane	6.06E+08	8.5
18.72	184.36	2,6-dimethyl undecane	1.68E+08	2.3
20.18	338.65	2-methyl tricosane	7.46E+07	1
20.38	170.34	2,6-dimethyldecane	1.60E+08	2.2
20.58	152.19	4-ethyl-2-methoxy phenol	6.46E+07	0.9
21.2	184.36	tridecane	2.78E+08	3.9
22.74	164.2	eugenol	3.36E+07	0.5
22.91			1.80E+07	0.3
23.2	212.41	trimethyl dodecane	2.82E+07	0.4
23.86	198.39	tetradecane	7.63E+07	1.1
25.24	164.2	isoeugenol	5.61E+06	0.1
26.38	212.41	pentadecane	1.25E+07	0.2
26.6	206.32	2,4-di-t-butylphenol	1.49E+07	0.2
28.59	224.43	hexadecene	9.63E+06	0.1

Table C2. Distillate Aqueous phase

R(t)	MW	Compound	peak area	Molar fraction (approx)
3.886	100.12	2,3-pentanedione	1.14E+08	0.1672
4.168	86.09	succinaldehyde	5.29E+07	0.0774
5.338	82.04	2-cyclopenten-1-one	8.92E+07	0.1305
5.509	116.16	diacetone alcohol	3.55E+07	0.0519
5.988	103.12	ethyl acetohydroxamate	4.49E+07	0.0657
6.239	116.12	acetoxyacetone	3.56E+07	0.0520
7.344	96.13	2-methyl-2-cyclopenten-1-one	3.02E+07	0.0441
7.51	84.07	2(5H)-furanone	1.04E+07	0.0152
7.562	86.09	butyrolactone	1.39E+07	0.0204
9.167	96.13	3-methyl-2-cyclopenten-1-one	2.91E+07	0.0425
9.515	96.13	2-methyl-2-cyclopenten-3-one	8.36E+06	0.0122
9.653	94.11	phenol	4.15E+07	0.0606
10.225	142.29	decane	5.77E+06	0.0084
11.04	112.13	methyl cyclopentenolone	2.39E+07	0.0350
11.412	110.17	spiro[2.4]heptan-4-one	5.39E+06	0.0079
11.981	108.14	2-methyl phenol	2.16E+07	0.0316
12.669	108.14	4-methyl phenol	2.12E+07	0.0309
13.025	124.14	2-methoxy phenol	4.68E+07	0.0684
13.62	156.31	undecane	5.20E+05	0.0008
16.154	138.16	2-methoxy-4-methyl phenol	2.94E+07	0.0431
18.597	152.19	2-methoxy-4-ethyl phenol	4.43E+06	0.0065
21.671	184.36	tridecane	3.02E+06	0.0044
24.609	206.32	2,4-di-t-butyl phenol	1.05E+07	0.0154
26.605	224.43	hexadecene	4.19E+06	0.0061
31.039	266.51	nonadecene	1.25E+06	0.0018
			6.84E+08	1.0000

Table C3. Pyrolysis oil light phase

Pyrolysis oil lights (in acetone)				
MW	RT	Compound	Area	% of Total
92.12	4.897	toluene	1.16E+07	1.3
90.12	5.37	butanedial	1.39E+07	1.6
116.16	6.983	4-hydroxy-4-methyl-2-pentanone	5.06E+07	5.7
106.17	7.609	ethylbenzene	5.19E+07	5.9
106.16	7.896	p-xylene	8.61E+06	1
118.17	9.004	2-butoxy ethanol	1.86E+07	2.1
94.11	11.572	phenol	1.52E+07	1.7
142.29	12.134	decane	8.45E+06	1
112.13	12.966	2-hydroxy-3-methyl-2-cyclopenten-1-one	1.35E+07	1.5
108.14	13.949	3-methyl phenol	7.80E+06	0.9
108.14	14.646	4-methyl phenol	1.59E+07	1.8
124.14	14.987	2-methoxy phenol	1.75E+07	2
138.16	18.14	creosol	2.16E+07	2.4
110.11	18.258	1,2-benzenediol	4.48E+07	5.1
144.13	18.905	1,4:3,6-dianhydro- α -D-glucopyranose	9.85E+06	1.1
124.14	20.941	4-methyl-1,2-benzenediol	5.31E+07	6
164.2	22.73	eugenol	1.27E+07	1.4
	23.06		5.46E+06	0.6
138.16	23.451	4-ethyl-1,3-benzenediol	3.02E+07	3.4
200.37	23.657	1-tridecanol	1.68E+06	0.2
152.15	23.945	vanillin	2.17E+07	2.5
164.2	25.236	2-methoxy-4-(1-propenyl) phenol	6.12E+06	0.7
166.17	26.133	1-(4-hydroxy-3-methoxyphenyl)-ethanone	1.17E+07	1.3
162.14	26.603	levoglucosan	1.94E+08	21.9
162.14	26.665	levoglucosan	2.52E+07	2.8
162.14	26.692	levoglucosan	1.11E+08	12.5
180.2	27.124	1-(4-hydroxy-3-methoxyphenyl)-2-propanone	8.11E+06	0.9
180.2	28.248	4-(3-hydroxy-1-propenyl)-2-methoxy phenol	5.95E+06	0.7
224.43	28.583	hexadecene	9.47E+06	1.1
182.17	29.945	4-hydroxy-3-methoxy benzeneacetic acid	1.15E+07	1.1
178.18	31.92	4-hydroxy-2-methoxycinnamaldehyde	1.05E+07	1

Table C4. Pyrolysis Oil Heavy phase

Pyrolysis Oil Heavy phase				
Mw	RT	Compound	area	%total
92.12	4.889	toluene	8.37E+06	0.3
96.09	6.765	furfural	5.93E+07	2.1
116.16	6.982	4-hydroxy-4-methyl-2-pentanone	6.24E+07	2.2
106.17	7.608	ethylbenzene	1.91E+07	0.7
94.11	11.560	phenol	5.90E+07	2.1
112.13	12.979	2-hydroxy-3-methyl-2-cyclopenten-1-one	6.16E+07	2.2
108.14	13.942	3-methyl phenol	4.54E+07	1.6
108.14	14.640	4-methyl phenol	1.05E+08	3.7
124.14	14.985	2-methoxy phenol	7.35E+07	2.6
122.16	16.884	2,4-dimethyl phenol	2.77E+07	1.0
138.16	18.142	2-methoxy-4-methyl phenol	1.07E+08	3.8
110.11	18.266	1,2-benzenediol	2.47E+08	8.7
124.14	20.101	4-methyl-1,2-benzenediol	9.04E+07	3.2
152.19	20.577	4-ethyl-2-methoxy phenol	4.65E+07	1.6
124.14	20.958	4-methyl-1,2-benzenediol	3.00E+08	10.6
164.2	22.730	eugenol	5.32E+07	1.9
138.16	23.468	4-ethylcatechol	2.09E+08	7.4
152.15	23.971	vanillin	1.68E+08	5.9
164.2	24.105	2-methoxy-4-(1-propenyl) phenol	6.17E+07	2.2
164.2	25.236	2-methoxy-4-(1-propenyl) phenol	1.68E+08	5.9
166.22	25.411	2-methoxy-4-propyl phenol	3.19E+07	1.1
152.19	25.815	4-propyl-1,3-benzenediol	1.05E+08	3.7
166.17	26.149	1-(4-hydroxy-3-methoxyphenyl) ethanone	1.06E+08	3.7
162.14	27.137	levoglucosan	1.76E+08	6.2
150.17	28.089	4-chromanol	8.34E+07	2.9
180.2	28.256	4-(3-hydroxy-1-propenyl)-2-methoxy phenol	4.54E+07	1.6
182.17	29.962	4-hydroxy-3-methoxyphenylacetic acid	1.04E+08	3.7
178.18	31.937	3-methoxycinnamic acid	1.81E+08	6.4

D. HPLC Results

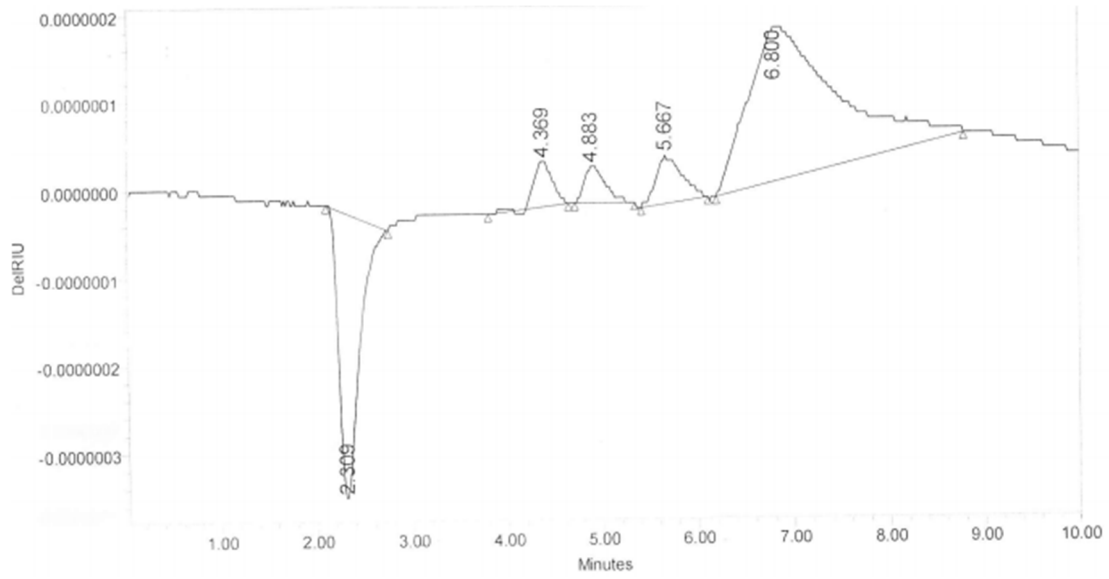


Figure D1. 100 ppm standard

Table D1. Standard retention times

Chemical	Average Retention Time (min.)
Formic acid	4.38
Acetic acid	4.9
Propionic acid	5.6
Butyric acid	6.8

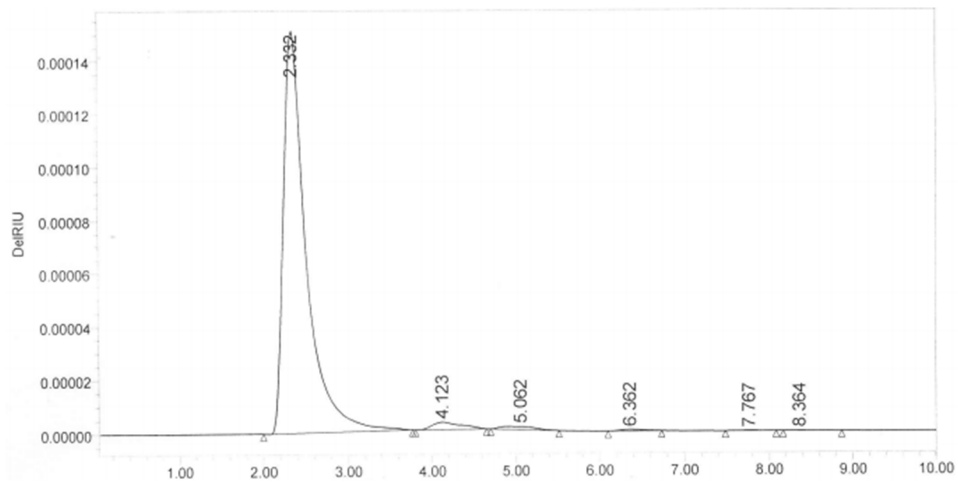


Figure D2. 97 hour AMX sample peaks

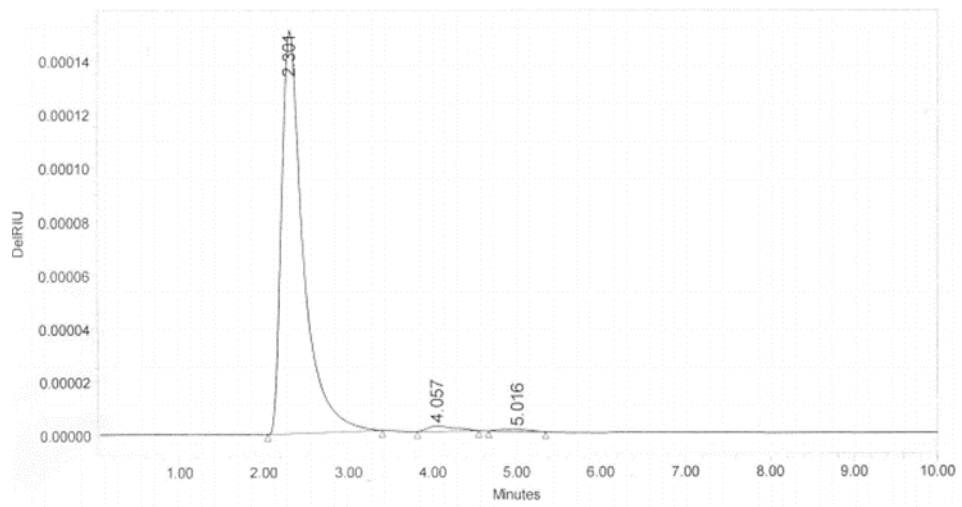


Figure D3. 97 hour CMX sample peaks

E. Sample Microscopies

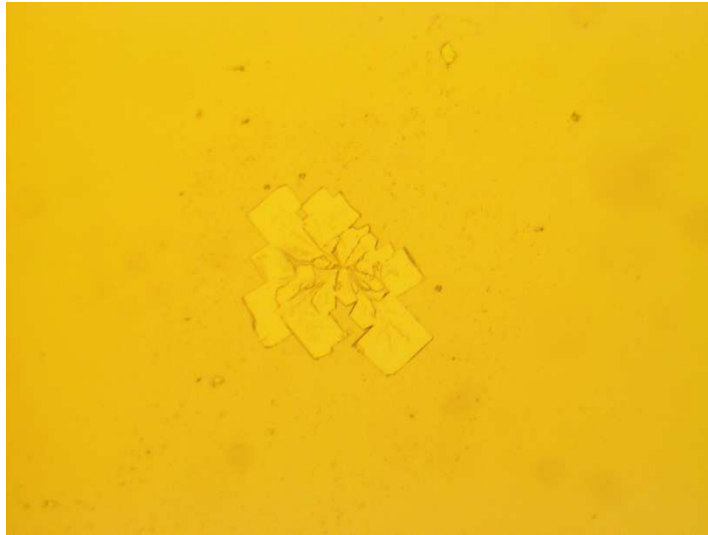


Figure E1. Initial sample slide (4x magnification)

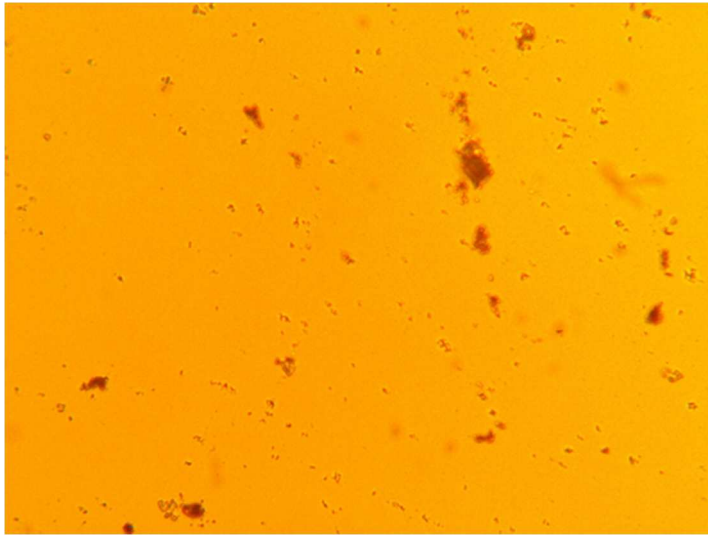


Figure E2. P5 CMX sample slide (40x magnification)

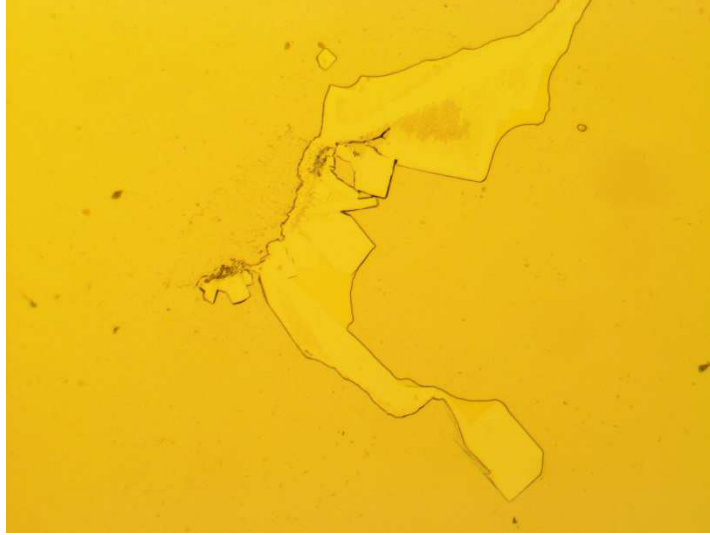


Figure E3. P5 AMX sample slide (4x magnification)



Figure E4. P7 AMX sample slide (10x magnification)

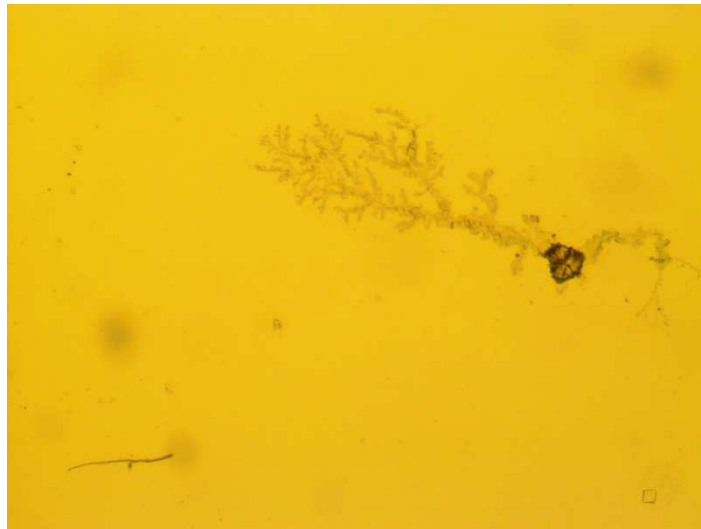


Figure E5. P7 CMX sample slide (4x magnification)

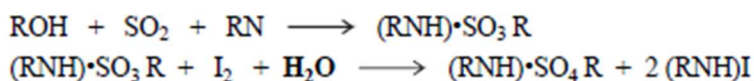
F. Karl Fischer Standard Operating Procedure (SOP)

This standard operating procedure (SOP) is for water content determination of liquid samples by means of a Mettler Toledo DL31 Karl Fischer titrator. This SOP is divided into three sections. The first gives general information about the titrator such as the reaction and terminology. The second gives a general function and overview of the buttons on the titrator, and the third section gives a general operation procedure and maintenance of the instrument. The titrant used in these examples is a one-component reagent. This SOP assumes the titrator is already assembled, if this is not the case the manual should be reviewed. The combititrant 5 one component reagent used for this measurement contains the following compounds: imidazole, iodine, sulfur dioxide, and diethylene glycol monoethyl ether.

General information

Operating principle

Water concentration of a sample is determined by the titrator when it detects a decrease in voltage below a set point called the end point. The current is held constant, but the resistance of the solution in the vessel changes with the changing water content as the titration proceeds. The general titration reaction for the Karl Fischer reaction is shown in Scheme 1 below.



Scheme 1. Titration reaction

The alcohol used is methanol and the base is imidazole. The iodine reacts with the water introduced with the sample and as long as there is water present, iodine will be absent, assuming adequate mixing. The resistance will increase compared to the iodine containing solution and so will the voltage required to maintain the specified polarization current at the electrode. Once all the water has reacted with iodine, there will be free iodine present which causes ionic conduction. Iodine molecule are attracted to the negatively charged electrode where it picks up two electrons, turning into iodide (2I^-), and carries them to the positive electrode. The ionic conduction reduces the resistance of the solution; therefore, the voltage is also reduced in order to keep the polarization current constant. Once the voltage drops below the specified endpoint, the titration is terminated and the moisture is determined based on the amount of titrant used.

Polarization current

The polarization current, end point, and the electrode size and type are all related. For a double platinum pin electrode with a 1 mm diameter and 3-4 mm length, the recommended end points related to polarization currents are shown below in table a. As a general rule of thumb, the larger the platinum electrode surface area, the smaller the potential jump.

Table a. End points related to polarization currents

I _{pol}	End point
1 μA	20 to 30 mV
5 μA	50 to 70 mV
10 μA	80 to 100 mV
20 μA	100 to 120 mV
30 μA	130 to 150 mV
40 μA	150 to 170 mV

Generally, as the polarization current is increased, the shorter the titration time, but the electrode also gets contaminated quicker which results in the need to be cleaned. The best time saving opportunities are by switching from 5 μA to 20 μA, after that, contamination increases and the titration time is not significantly improved.

Stirring speed and dispersion of titrant

For the titrator to produce accurate results adequate mixing is required for homogenization of the sample/solvent mixture. Generally, the optimum stirring speed is achieved when a small vortex is visible. If the speed is too high, bubbles may form which cause fluctuations in the resistance of the medium the current is passed through leading to inaccurate results. On the other hand, a stir speed that is too slow may also give false results due to overtitration. The titrant feed tube should also be placed at the maximum spot of turbulence; this is shown in figure 1 along with a vortex picture to indicate appropriate mixing speed.



Figure 1. Appropriate mixing for titration

NOTE: Stirring speed may be adjusted in between samples while on standby mode. Click the ‘stirrer’ button and change to desired speed, then click ‘OK’.

Learn Titration option

This option may be accessed by the pressing the red “i” button while on the home screen. This may be used to determine the optimum titration parameters for a sample type. This requires only four inputs: method number (which the parameters will be saved in), type of sample, result unit, and titrant type. Once the titration takes place, the following results are given: sample water

content, optimum ΔV_{\max} , ΔV_{\min} , ΔV_{\max} factor, and relative drift stop, and limits for amount of sample to titrate. If no endpoint is detected, the titration is terminated after two full burettes of titrant are used.

NOTE: Only one user defined method may be saved in the DL31 titrator

Termination parameters

Generally, the relative drift stop should be chosen as a termination parameter since it is independent of titrant concentration and initial drift. The first parameter considered to terminate the titration is the end point. Once the endpoint is reached, the termination drift conditions must be satisfied for the duration of the delay time specified to terminate the titration. If absolute drift is chosen as a termination parameter the drift detected by the titrator must reach the value specified (30 $\mu\text{g}/\text{min}$ recommended) for the duration of the delay time. A disadvantage of using the absolute drift stop is that the drift stop value must be higher than the initial drift since it must come back to or below the absolute drift stop value. If this is not the case the titration termination will not be reached and instead another parameter such as a safety parameter, such as max volume or max time, will be used for termination. For the relative drift termination parameter, the drift must at most reach the addition of the drift value detected when the titration started and the value specified. For the one-component reagent, a relative drift stop of 10 to 15 $\mu\text{g}/\text{min}$ is optimum for achieving reproducibility, any higher there is risk in obtaining high error measurements. The relation between drift and reproducibility/accuracy of results are that the lower the drift the better the reproducibility but the longer the titration. The higher the drift the lower the reproducibility but the titration proceeds faster.

Terminology

A summary of terms and definitions used by the titrator is displayed below in table b.




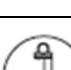

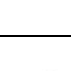




Table b. Summary of terms and definitions

Ipol	Polarization current is the current supplied to the electrodes
ΔV_{\min}	Smallest addition increment of titrant in μL per 0.1 seconds. It must be large enough to compensate for the drift.
ΔV_{\max}	Largest addition increment of titrant in μL per 0.1 seconds
ΔV_{\max} factor	used for 2-component titrants to avoid overtitation. Should be set to 100% for one-component reagents.
Drift	The total ingress of water into the titration stand during a defined period of time ($\mu\text{g H}_2\text{O}/\text{min}$).
Abs. drift	The value of the abs drift must be larger than the pre-defined drift. Typical absolute drift stop value = 30 $\mu\text{g}/\text{min}$.
Rel. drift	The typical relative drift stop value = 20 $\mu\text{g}/\text{min}$
Start: Cautious	This starts titration by adding smallest amount set (V_{\min}) and then increasing linearly to maximum amount (V_{\max}) in about 20 seconds if needed. This is recommended for samples with water less than 100 μg , but may be used with any sample though it may increase titration time.
Delay time	Time in which the voltage remains below an endpoint defined value. This is used as a termination parameter sometimes. (typical value of 15 seconds)

Buttons

Table c below summarizes the general function of the buttons found on the panel of a DL31 Karl Fischer titrator.

Table c. Button and function summary

<u>Key</u>	<u>Function</u>
	Provides access to the value of the current solvent capacity, last drift determination, "Hello" Karl Fischer tutorial, and menu for testing titrator hardware.
	You can switch the stirrer on and off and change the stirrer speed when the titrator is on standby mode
	This button is used to either siphon off solvent or add it by pressing the blue rubber button with the same logo while the pump is running
	This button is used to rinse the burette, rinse the tip of the dispensing tube, and also add a specified amount of titrant to the reaction vessel if need be.
	Resources required for titration such as the titrants and standards are stored in the setup menu and can be changed
	Results are determined by the use of a method (a set of operating parameters used by the titrator). All the methods can be accessed by this button and can be changed. The resources defined in the setup menu are available for these methods
	This button is used to perform a titration. The method called determines the analysis sequence
	The results list of samples analyzed may be viewed by pressing this button. One may also perform recalculations, and print out additional reports (if printer is available)
	Changes in the current menu or submenu are discarded and the original values/names remain in force. This key always effects a return to the previous display
	Used to terminate analyses or other actions. Data that are not stored are lost

General procedure

The following notes should be considered while performing the reaction in order to obtain accurate results.

- Ensure the titrant dispensing hose tip has an anti-diffusing tip in it before starting the titration.
- Concentration of titrant (especially for one-component reagents) must be determined every day a titration is done.
- Volumetric Karl Fischer titrators (DL31/38) have a 50 ppm detection limit.
- The Maximum speed of the Karl Fischer reaction is reached in the pH range of 5.5 to 8.
- If acidic or basic samples are analyzed, buffering agents must be added to the solvent to ensure the titration is quick and without side reactions. Imidazole for acidic samples and salicylic or benzoic acid for basic samples.
- 30-70% of burette volume of titrant should be used per sample to obtain most accurate results (Aim for 50%). The optimum amount of water in a sample is 10 mg.
- Stirring speed must be just right to obtain accurate results. If bubbles form it is too fast and if no vortex is seen then the speed is too slow.
- Titration may be terminated other parameters such as max time or max amount of titrant dispensed, these are set by the user.
- Normal stable drift values for this titrator is less than 5 $\mu\text{g H}_2\text{O}/\text{min}$. This may be obtained by shaking the titration vessel periodically while in pre-titration step, and making sure the vessel is airtight.
- Desiccants have a limited life and are exhausted after 2-4 weeks. The silica gel can be regenerated at 150°C and the molecular sieve up to 300°C.
- Titrant concentration has proven to change by 0.1 mg/mL per week, for this reason weekly concentration determinations are stated to be sufficient by the manual, but daily determinations are better.
- Solvent should be changed when the standard concentration determination is 5% or greater than the printed value on the test certificate.
- Titration may be affected by temperature, consult manual if titration is performed in temperatures above 30°C.
- Aldehydes and ketones are a special case and may give false readings when used with methanol containing reagents, the manual should be consulted for reagent modification.
- **See application brochure 26 page 27 for notes on sugar samples.

Procedure

The general procedure assumes that the standard and samples are already prepared into the appropriate syringe with a needle. The standard chosen for this procedure is the Hydranal 10.0, though other standards may be used with slight modifications to the procedure. It is also assumed

that the moisture content is determined by weight difference. This means that the titrator will ask for amount of sample introduced into the vessel as a weight value; therefore, both the standard and sample syringes must be tared on a mg range analytical scale and the difference in weight is the value that will be entered for the weight of the sample.

1. Turn on titrator by the ON switch located on the behind the instrument on the lower left hand corner (facing the titrator keypad)
2. To make a method (set of parameters for titration) press method and input the desired parameters. General parameters for different titrants are shown below in table b.

Table b. General parameter values for different titrants

Titration type	I _{pol} μA	EP mV	ΔV _{min} μL	ΔV _{max} μL	ΔV _{max} factor %	Rel. drift stop μg/min
One-component	20	100	0.5	4.0	100	15
Two-component	20	100	0.5	8.0	30	15
Pyridine-cont. (one-comp.)	20	100	0.5	3.0	100	15

**The learn titration option may also be used to obtain optimum parameter values for a specific sample. This is accessed by pressing the <i> button and clicking the learn titration option.

3. To rinse the burette, disconnect the titrant delivery tube from the vessel and place in the waste container. Press the <burette> button and make sure the 100% dispense number is displaying. Then click start with a function key and allow the titrant to be disposed into the waste container, do this three times. Then reconnect the titrant delivery line to the titration vessel. DO NOT RINSE BURETTE IN TITRATION VESSEL.
4. Make sure the waste suction tube is lifted to the top of the vessel, then click the <Pump> button, then 'start' with a function key. The pump motor should start, then press on the rubber blue button perpendicular to the ground in front of the titration vessel to deliver solvent into the vessel. If no solvent (methanol) is being delivered into the vessel, make sure the solvent bottle is not empty, then check the fittings and connections to ensure all lines are sealed. The vessel should be filled to the 40 mL mark on the vessel.
5. If method is already created, then press the <Run> button and go through the options adjusting any values if needed. Upon clicking 'OK' for the last option then the pre-titration will start. To aid in the pre-titration (depletion of water in vessel) the vessel should be shaken periodically.
6. Once the pre-titration has stabilized at a value lower than 5 μg/min (or with a → arrow on the screen), the 'CONC' option should be clicked with a function key to determine the concentration of the titrant. Select 0 for the mixing time and the weight of the sample should be left blank until the end of the titration, click 'OK'. When the screen prompts to

enter a certain amount of sample, insert approximately 1 mL of standard into the vessel through the syringe opening and click OK.

NOTE: The time the vessel is opened to the atmosphere should be minimized.

7. Once the titration is done the titrator will ask for the weight of sample, enter the weight in grams using the number keypad, then select 'enter' with a function key.
8. The titrator will now go back to standby mode, wait for the drift to be stable and as low as possible. ($< 5 \mu\text{g}/\text{min}$)
9. Tare the scale while the syringe with the standard is on it. Then press "sample" on the titrator with the appropriate function key.
10. Knowing the relative concentration of the sample will facilitate the titration and possibly speed it up. If known enter it on the "H₂O exp." row. Then enter 0 for the weight of the sample (sample weight should be entered after titration). No guess is required.
11. The screen will then prompt to enter an amount determined using the guess value.
12. Remove the stopper and inject the sample into the vessel pressing the "enter" button and using the putting the stopper back on. The amount of time the stopper is removed should be minimized.
13. Place the syringe back on the scale to obtain the weight of the sample injected, wait for the end of the titration. Titration should consume ~50% of the burette volume. If more than this then lower sample amount next time, if lower than this then increase the amount of sample on the next sample run.
14. Once the titration is done the weight of the sample will be required. If the % result option was chosen from the parameters then the concentration will be displayed in % by weight. If not then other units may be used such as ppm etc.
15. The value should not have a deviation greater than 5% than the value printed on the test certificate.
16. To analyze samples repeat steps 9-14 using the syringe with the sample instead of the standard.
17. The amounts of samples should be recorded to optimize the amount titrant used and minimize sample determination redo.
18. Solvent saturation differs from sample to sample; therefore, the standard should be used to test the solvent by subjecting ~1 mL of standard to titration after every few sample titrations. If the value given by the analysis is within 5% from the value given in the test certificate the solvent may be used (though one may have to adjust the mixing speed as the volume increases). If the value has an error of 5% or greater, then the solvent must be changed in order to keep obtaining accurate measurements.
19. The titration vessel should be rinsed with the solvent (methanol) a couple of times in between changing the solvent.
20. Once the titration is done the vessel should be rinsed with methanol and the electrode should be wiped with a non-lint leaving paper towel wet with methanol being careful not to bend the electrodes.
21. Press the <reset> button and turn off the titrator using the button on its back side.

Maintenance

The following are tips to prolong the life and reliability of the Karl Fischer titrator as an analytical instrument.

- In the case of clogging, the instrument should be disassembled and the hoses should be rinsed with methanol, water, and then air dried with dry air or another inert gas.
- The gaskets should be replaced periodically; meaning every couple of years or when needed.
- The anti-diffusion tip should be replaced when/if clogged.
- Clean the vessel and electrode after every use.